Federal State Autonomous Educational Institution of
Higher Education
"SIBERIAN FEDERAL UNIVERSITY"
School of Petroleum and Natural Gas Engineering
Department of Chemistry and Technology of
Natural Energy Carriers and Carbon Materials

APPROVED
Head of the Department
_____ Fedor A. Buryukin
«_____» _____ 2021 г.

MASTER'S THESIS

Investigations of Asphaltenes' Structure and Properties of West Siberian Crude Oils

04.04.01 Chemistry
04.04.01.05 Petroleum Chemistry and Refining

Research supervisor   Candidate of   Vladimir Safin
                                        Chemical Sciences,
                                        Associate Professor

Graduate   Asamoah A. Abraham

Krasnoyarsk 2021

ABSTRACT

Asphaltene molecules are solid crude oil constituents that are complex compounds with high molecular weight and varying structures that contain metal complexes. These solid molecules are homogenised as part of crude oil by resins which encapsulate them to form micelles. However, these micelles when destabilized, lead to asphaltene precipitating into their solid state and cause severe operational and transportation problems of crude oil such as catalyst deactivation. This research seeks to scrutinise the complex structure of asphaltenes contained in Western Siberian Oils and how these molecules affect the properties of the oils.

Owing to the diverse structures asphaltenes possess, asphaltene structure has been modelled using different models. These models are discussed. Asphaltene molecules isolated from different sources have different structures.

There are various analytical methods applied in characterization of asphaltenes however SARA analysis and infrared spectroscopy were employed in ascertaining the structure of these molecules and the relationship with the crude properties explained.

TABLE OF CONTENTS

INTRODUCTION

Cholesterol is a waxy, fat-like substance that is found in blood. It is essential to the body because the body requires some cholesterol to create hormones, vitamin D, and substances that aid in digestion of food. However, cholesterol is additionally found in foods from animal sources, such as egg, meat, shellfish and cheese. Although cholesterol is vital, if there is excessive cholesterol in the blood, it can combine with other substances in the blood to form a plaque. This process is termed atherosclerosis. This plaque sticks to the walls of the arteries and can lead to coronary artery disease, where the coronary arteries become narrow or even blocked.

Asphaltene is known as the cholesterol of petroleum because of its ability to precipitate, deposit, and as a result, interrupt the continuous production of oil from underground reservoirs [19].

They were first defined as the "distillation residue of bitumen insoluble in alcohol and soluble in turpentine."[6] However, this definition was later adapted owing to an error in the initial definition, which limited asphaltene presence to bitumen and was later found to be incorrect [13]

Asphaltenes have been reported to be problematic during recovery, transportation and processing of crude oil and their destabilization can lead to variations in crude properties. These problematic crude constituents have not been fully characterized. However, definitively, asphaltenes are polar, polyaromatic high molecular weight hydrocarbon fractions of crude oil that are soluble in light aromatic hydrocarbons but insoluble in low molecular weight paraffins such as n-pentane and n-heptane [7, 16, 28, 41]. They may also comprise of significant amounts of heteroatoms, including oxygen, sulfur, nitrogen, and metals, which could cause severe operational problems during diverse stages of oil and gas production [45].

The complexity of asphaltene molecules comes primarily in the way its structure is defined. There are several different asphaltene structures, which makes generalizing it into an explicit family very difficult. However there are models that are used to describe asphaltene structure. Asphaltene can be considered as continental or archipelago. Nevertheless, currently, the widespread model for asphaltene is the Yen model. This model's description of asphaltene structure is established on size and behaviour as a function of the crude oil in which the asphaltene is contained.

Unlike some other crude constituents, asphaltenes are solids. These solids constituents are homogenized in crude oil by resins the subsume them to form micelles. However, changes in reservoir or pipeline conditions such as temperature and pressure may cause these asphaltenes to precipitate. After precipitating, they aggregate to form dense flocculation which then deposit themselves into reservoir pores, wellbores or pipelines thus causing decrements in flowrates which as a result of decrement in diameter of the pipelines, wellbores or reservoir pores.

The problems asphaltenes pose have been observed in all stages of oil production and processing, in near wellbore formations, production tubing, surface facilities and refinery units.

Much research has been carried out on the properties of Western Siberian crude oils however this research seeks to explore the structure of asphaltenes and how they influence the properties of oils from these oilfields. Asphaltenes have been reported to be problematic during recovery, transportation and processing of crude oil and their destabilization can lead to variations in crude properties.

Figure 1 - Pipeline diameter reduced by asphaltene agglomeration thus reducing oil flow in the pipeline (left) and Coronary artery diameter reduced/almost blocked by plaque formed from cholesterol thus reducing blood flow (right).

2.0 Main components of crude oil

Crude oil, is a complex liquid mixture that occurs naturally which comprises mostly of hydrocarbons, but also contains some compounds of oxygen, nitrogen and sulphur. Compared to coal, the elemental composition of crude is much less variable: 82.5 - 87% carbon; 11.5 - 14.5% hydrogen; 0.05 - 0.35, and sometimes but infrequently, up to 0.7%, oxygen; up to 1.8% nitrogen and up to 5.3% - 10%, Sulphur. There are also traces of metals such as Ca, Mg, Fe, Al, Si, V, Ni, Na, etc., which are considered as impurities and are detrimental to refining processes and product contaminants.
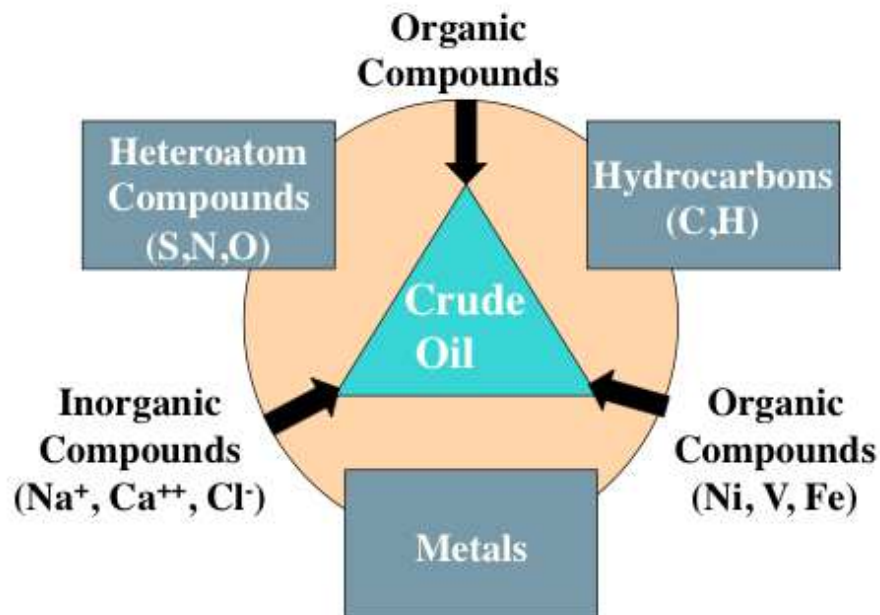
Figure 2 - Composition of Crude Oil

The composition of crude is broadly classified into Saturates, Aromatics, Resins and Asphaltenes and this is widely abbreviated as SARA. The resin fraction and the oil fraction (Saturates and Aromatics) are collectively referred to as Maltenes. Maltenes can be considered as n-pentane or n-heptane soluble fraction of petroleum with relatively high boiling point (>300°C, 760mm). However, a combination of Saturates and Aromatics is known as Petrolene which is defined as the part of n-pentane or n-heptane soluble fraction with a relative low boiling (<300°C, 760mm) and can be distilled without thermal decomposition. Each of these components are described below and their relation to the asphaltene is explained.

2.1.0 Saturates

Saturates (alkanes) also known as paraffins are hydrocarbons that do not have multiple bonds between carbon atoms. Thus, the tetravalent carbon atoms are bonded to

the maximum allowable hydrogen atoms. The general formula of Alkanes is C_nH_{2n+2} and the simplest alkane compound is methane, followed by ethane and propane [13].
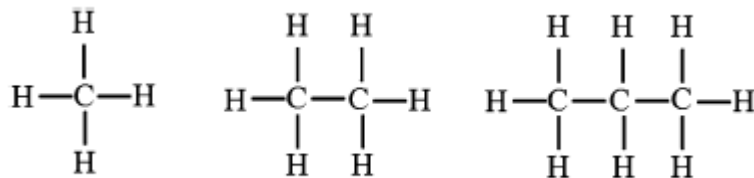

Figure 3 - Molecular structure of methane, ethane, and propane [12]

Saturates are one of the chief liquids, or gas with regards to C_1-C_4 saturates, components of petroleum. Asphaltenes are in solution within these compounds until they are destabilized and then begin to precipitate. At the moment, saturates are known to play no role in asphaltene stability that is noteworthy.

2.1.1 Aromatics

The second major component of petroleum is Aromatics. Juxtaposed to saturates, aromatics have a more complex structure. Generally, aromatics are nonpolar and are characterized by an unsaturated hydrocarbon ring with multiple carbon–carbon double bonds within the ring configuration [2, 3, 20, 25, 36, 37].
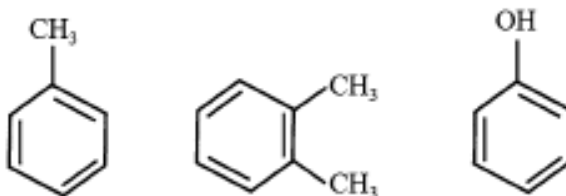
Figure 4 - Structure of simple aromatics

2.1.2 Resins

The complexity of the structure of resins is much higher in comparison thereto of saturates and aromatics. Resins are polar and also have a high molecular weight (500 to 1000 amu), as compared to the formerly mentioned constituents. There has been much less stress on the resin fraction of petroleum. Additionally, the resin fraction can contain components of equal polarity to the components of the asphaltene fraction. They also form high yields of about 35% by weight of thermal coke and contribute to catalyst deactivation as much as the asphaltene fraction. Resins are insoluble in liquid propane but soluble in n-heptane. It is the resin fraction that ostensibly is extremely significant in relation to the

structure and stability of petroleum by averting the separation of the molecules of the asphaltene fraction or part of this fraction into a separate phase.

Crude oil, generally, is nonpolar, which implies it is insoluble in water [24]. Asphaltene, unlike the other constituents of crude, is highly polar in nature and therefore cannot be homogenized or solubilized within crude oil on its own. Characteristically, resins have both polar and nonpolar ends and consequently function as a bridging entity that unites the nonpolar hydrocarbon compounds to the highly polar asphaltene [26]. The resin molecules encapsulate asphaltene molecules to form asphaltene clusters known as micelles and thus suspending them in liquid oil. These micelles are responsible for the conservation of the colloidal stability of petroleum insofar as the asphaltene constituents continue to be dispersed in the crude oil and the whole exists as a stable system. This results in higher resin content than asphaltene because each asphaltene is enclosed by a number of resin molecules.

In a pure state, resins are either heavy, viscous liquids or sticky solids. They are also as much volatile as other hydrocarbons of the same molecular size.

The basic structure of resins and asphaltenes are similar except that the napthenic systems may be higher in resins as compared to asphaltenes or there may be a higher degree of substitution by paraffinic chains on the aromatic nuclei of the resin constituents. Both of them are formed by the oxidation of polycyclic aromatic hydrocarbons. Perhaps asphaltenes may be mature resins. If so, then the maturation of resins into asphaltenes involves aromatization of non-aromatic systems of the resins. Both resins and asphaltenes cannot be defined by their chemical constituents but are defined operationally by the method of separation.

Figure 5 - Molecular structure of simple resin molecule [1]
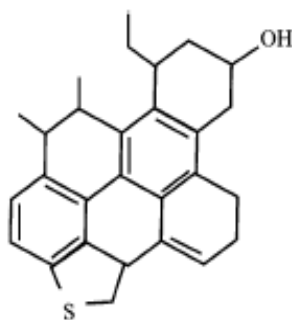
2.1.3 Asphaltenes

Asphaltenes are solids without a certain melting point. They are dark-brown, friable and typically leave a carbonaceous residue on heating. Asphaltene, undoubtedly, is one of the most complex constituents of crude oils. They comprise of condensed polynuclear aromatic layers joined by saturated links. Asphaltene molecules are composed of about 10

to 20 pre-condensed aromatic rings which carry naphthenic and paraffinic groups remaining in the form of aggregates that also have the propensity of forming complexes with metals like vanadium and nickel.

Asphaltene is one of the very few solid crude oil constituents. The complexity of asphaltene molecules comes primarily in the way its structure is defined. All three aforementioned constituents have general structures by which they can be classified. Unfortunately, asphaltene has numerous dissimilar structures, which makes generalizing it into a specific family very difficult [34]. Nonetheless, because of its insolubility in n-alkanes, asphaltene is usually classified as a solubility class. Certain characteristics that can be employed in the identification of asphaltene molecules include [40]:

- Solid: Asphaltene, unlike most crude constituents, is in the solid phase but is engulfed and homogenized in the petroleum by resins at reservoir conditions.

- n-alkane insoluble: This classification emphasizes on the fact that asphaltenes are insoluble in light n-alkanes and due to it possessing several dissimilar structures, it can be categorised as a solubility class rather than a general structure which makes classification cumbersome. Consequently, they can be defined as the constituent of crude oil with the highest molecular weight that is insoluble in light n-alkanes such as n-pentane or n-heptane and soluble in aromatics such as toluene.

- Highly polar: Asphaltene is one of very few components of crude oil that is highly polar, in contrast to crude oil as a whole, which is considered nonpolar.

- Heteroatoms: Asphaltene is associated with heteroatoms that is chiefly manifested in oxygen, nitrogen, and sulphur as well as metals.

The densest portion of the crude oil is comprised of asphaltenes.

In the laboratory, asphaltenes are isolated from crude oil using non-polar solvents such as n-pentane and n-heptane. However, n-heptane is preferred over n-pentane because it excludes from the asphaltene precipitate any material that may be semisolid. Liquefied petroleum fractions (propane and butane) are industrially used in deasphalting residues and lube stock oils.

It is imperative to be able to distinguish between the different constituents of crude oil and isolate each constituent from the other to both quantify the components and individually study each constituent. Understanding the structure and chemistry of the constituents gives rise to an improved understanding of processing, transportation, storage and usage of crude oil and its products. Based on this, the most ubiquitous method used in differentiating between saturates, aromatics, resins, and asphaltene is referred to as the SARA analysis.
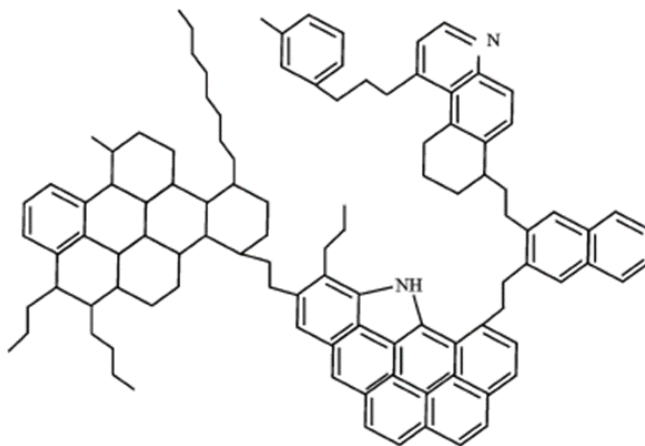
Figure 6 - Molecular structure of an asphaltene [16]

2.2 Molecular structure of asphaltene

Asphaltene, as can be seen figure 6, is mainly composed of compact poly-aromatic cores with long or short aliphatic chains and porphyrin molecules, different functional groups and heteroatoms. It is the most polar fraction of crude oil. There have been a lot of controversies about the structure and science of asphaltene.

Although it has been difficult to totally understand the chemical structure of asphaltenes, the average composition of asphaltenes as a class is fairly well-known. The simplest feature of any chemical compound is its elemental composition. Elemental analysis of asphaltene have shown them to be composed of carbon and hydrogen in an approximation of 1 to 1.2 ratio of carbon to hydrogen, compared to the 1 to 2 ratio for bulk alkanes. Dissimilar to the other hydrocarbon constituents of petroleum, asphaltenes is characteristically made up of a few percent of other atoms, called heteroatoms, such as nitrogen, oxygen, sulphur, nitrogen, vanadium and nickel. As concerns the structure of asphaltene, there is concordance among specialists that some of the carbon and hydrogen atoms are bound in a ring like, aromatic groups, which are also comprised of the heteroatoms. Paraffinic chains and cyclic paraffin contain the carbon and hydrogen atoms left and are linked to the ring core.

In this framework, asphaltenes demonstrate a range of molecular weight and composition. This compositional characterization is recognized by virtually all asphaltene specialists. However, there is ample room for debate about the structure or size of single asphaltene molecules.

2.2.1 Elucidating asphaltene structure by ^{13}c nuclear magnetic resonance

Nuclear Magnetic Resonance is a superb method by which the molecular structure of asphaltenes can be characterised. Several research groups have utilized NMR in asphaltene characterization.

^{13}C NMR is applied to characterize asphaltene. The spectral analyses of ^{13}C NMR are similar in manner as ^{1}H NMR spectra in that, often, analyses are made by dividing into several sub-regions. The ^{13}C NMR experiments often provide complementary data and ^{13}C chemical shift dispersion (0 – 220 ppm) incorporates a range wider than ^{1}H (0 – 15 ppm). This helps with the identification of functional moiety of asphaltenes. In the ^{13}C spectrum, the first sub-region of interest is between 5.00 ppm and 23.00 ppm. In this sub region, the ^{13}C peaks are allotted primarily to either terminal or branched $-CH_3$ groups. They are also allotted partially to $-CH_2$ in hydro-aromatic and naphthenic fragments. Particularly, terminal $-CH_3$ on aliphatic chain with a minimum of 3 or more carbons have signals around 14.20 ppm, whereas the peaks of branched CH_3 (β or more from terminal $-CH_3$) and terminal isobutyl CH_3 appear around 19.80 ppm and 22.80 ppm respectively. The resonance of $-CH_3$ groups in ethyl-substituted cyclohexane is between 11.00 ppm and 12.50 ppm, and also the resonance of methyl substituent on aromatic (unshielded by one aromatic) ring is about 21.30 ppm.
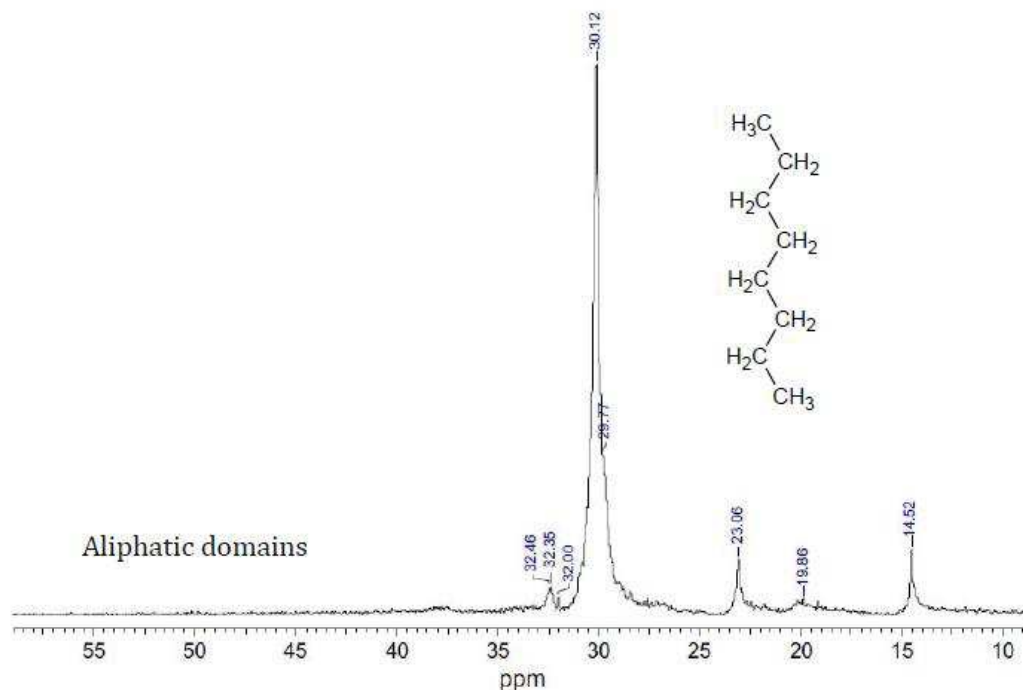

Figure 7 - Image depicting the aliphatic ^{13}C NMR region of an asphaltene Sample

There is the possibility to distinguish the aliphatic $-CH_3$ groups by analysing their ^{13}C NMR peaks (Table 1). As can be seen in Table 1, signals between 11.50 ppm and

14.20 ppm indicate –CH$_3$ in an aliphatic chain with a minimum of 3 or more carbons; 19.80 ppm denote branched –CH3, β or more from end of chain; and 22.80 ppm arising from terminal isobutyl (CH3)

Table 1 - Peak regions and assignments for ^{13}C NMR of asphaltene

13C NMR peak ranges (ppm)	Functional Group
11.00-18.00	terminal CH$_3$ on aliphatic chain with at least 3 or more carbons
18.00-20.00	branched CH$_3$, α or more from terminal CH$_3$
20.00-22.00	CH$_3$ substituent on aryl ring
22.00-24.00	terminal isobutyl CH$_3$; and possible CH$_2$ α to terminal CH$_3$
24.00-25.00	alicyclic ring beta to aromatic ring
25.00-29.70	aliphatic chain CH$_2$ positioned more than α or β to aromatic ring
29.90-31.90	alicyclic CH$_2$ (naphthenic)
32.00	CH$_2$ beta to t-CH$_3$ or aromatic ring
32.80	aliphatic CH
33.00-39.50	CH$_2$ or CH α to aromatic ring, CH$_2$ α to branched point in chain
40.00-55.00	α carbon to carboxylic group (porphyrins) / alicyclic (naphthenic) CH/CH$_2$
60.00-78.00	paraffinic and naphthenic carbon α to OH
110.00-120.00	aromatic carbons
121.00-124.00	bay type carbons
122.90	triple bridgehead (peri-condensed) quaternary aromatic carbon
125.00-129.00	fjord type carbons
127.00	aromatic protonated carbon
136.40	double bridgehead (cata-condensed) and substituted quaternary aromatic carbon
137.00-140.50	α carbon to sulfur or nitrogen atom in benzo, dibenzothiophene type structures
137.00-160.00	aromatic carbons without any proton
160.00-175.00	ester or amide carboxy carbon atom
178.00-190.00	quinolinic carbons
190.00-220.00	aldehydic and cetonic carbons

The second sub-region of interest is sited between 22.50 ppm and 37.00 ppm. There are two types of signals in this region. These signals arise from CH$_2$– and >CH– groups: CH$_2$ and CH groups in naphthenic fragments, and CH$_2$ groups of aliphatic chains. Signals

around 24.50 ppm denote alicyclic CH_2, which is β to aromatic ring and alicyclic CH_2 at more than β position to the nearest aromatic ring has a resonance at about 29.90 ppm. However, aliphatic CH_2 of naphthenic fragments located further from the aromatic core leads to a ^{13}C resonance around 32.80 ppm.
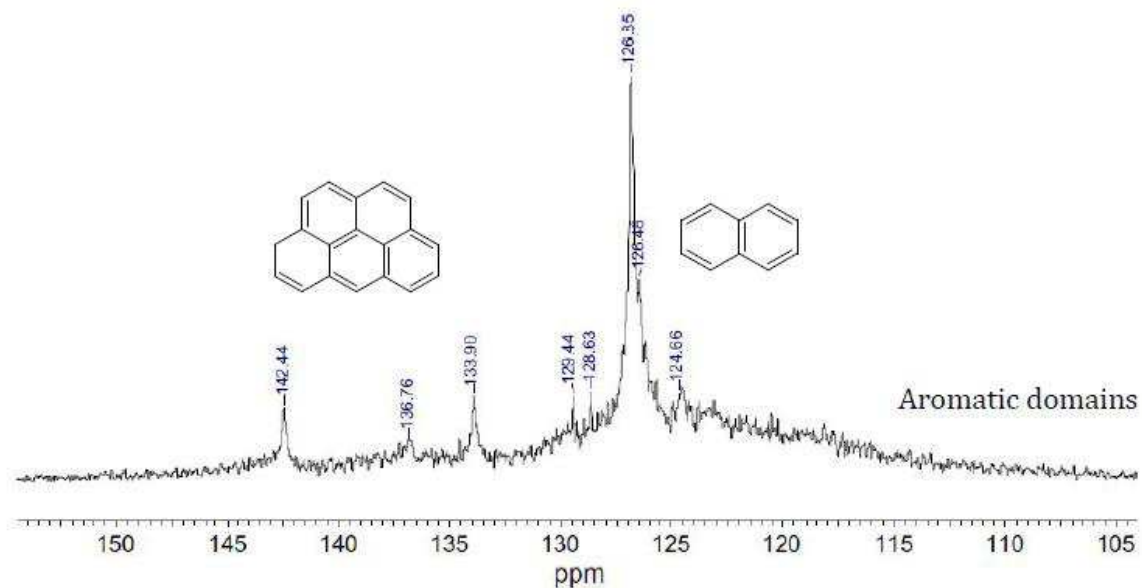
Figure 8 - Image showing the aromatic region of ^{13}C NMR spectrum

In both sub-regions of the ^{13}C NMR spectra of asphaltene samples, the resonances at 14.40 ppm, 23.10 ppm 29.60 ppm, 29.90 ppm, and 32.10 ppm are allotted to straight chain hydrocarbons while the signals around 19.70 ppm, 25.00 ppm, 27.50 ppm, 32.80 ppm and 37.50 ppm denote branched alkyl hydrocarbons. CH_2 groups belonging to aliphatic chains that are beyond α or β positions to aromatic ring give signals around 27.20 ppm and 29.50 ppm. The peak of CH_2 groups β to terminal CH_3 or aromatic is around 32.00 ppm while CH_2- groups α to either an aromatic ring, or at α position from a naphthenic ring, or to branched position in chain leads to the signal(s) around 37.00 ppm. Signals between 37.00 ppm and 60.00 ppm denote >CH– groups of naphthenic fragments of asphaltenes. Aliphatic carbons in ethers, alcohols and methoxy groups yield signals 53.00 ppm and 104.00 ppm and rings linking methylene, and >CH– in alkyl groups, and naphthenic rings have signals between 37.00 ppm and 53.00 ppm.

Studies by Poveda-Jaramillo et al. on asphaltenes from Colombian Colorado light crude oil reported ^{13}C NMR signals detected between 60.00 ppm and 78.00 ppm, which are assigned to paraffinic and naphthenic carbon α with OH groups [35]. Rakhmatullin et al. in another study of crude oils from Bashkortostan and Tatarstan fields observed ^{13}C NMR signals between 108.00 ppm and 118.00 pm which denotes olefin (alkene) fragments [38].

2.2.2 Elucidating asphaltene structure by Fourier-transform infrared spectroscopy (FTIR)

Infrared spectroscopy, due to the ideal range of wavelengths, is among the foremost versatile methods for studying the structure of chemical compounds. Infrared emission with a frequency of less than $100 \, cm^{-1}$ is absorbed by an organic molecule and is converted into the energy of its rotation, and radiation within the range of about $10,000 - 100 \, cm^{-1}$ is converted into the energy of vibrational motions of atoms in the molecule.

Fourier-transform infrared spectroscopy (FTIR) is a technique which can be used to evaluate functional groups present in the molecular structure of asphaltene that mainly occur within the $400 - 4000 \, cm^{-1}$ frequency range. The Hydrogen stretching region of FTIR spectrum is found in the $2500-3700 \, cm^{-1}$ interval. This inference is as a result of the vibration frequencies of C-H, N-H and O-H appearing in this area. The $2000-2300 \, cm^{-1}$ interval is denoted to the Triple Bond Stretching Region because $C{\equiv}C$ and $C{\equiv}N$ bonds are in this region. The $1600-2000 \, cm^{-1}$ range is assigned to the Double Bond Stretching Region, because the bonds C=C, C=N and C=O are located in this region. The $1000-1600 \, cm^{-1}$ interval is termed the Fingerprint Region, because several bonds such as C-O, C-N, C-C (single bonds), CH bending bond and some benzene ring bonds that define the type of functional groups are located in this area. The last interval within the FTIR spectra is the aromatic region, which can be found from $400–1000 \, cm^{-1}$ in which aromatic bonds are exhibited.

2.3 Models of asphaltene structure

Asphaltene structure is extremely complex. Typically, it is classified in a solubility class instead of a specific structure due to the many variations of structures available for asphaltene. However, owing to the complexity of the problem, models have been proposed in an effort to provide a comprehensive and standard system that would be able to befittingly describe all the dissimilar asphaltene chemical structures.

2.3.1 Archipelago model
This model of asphaltene molecular structure, like its name suggests, proposes the structure of asphaltene as several aromatic cores connected together by aliphatic chains. An example of an asphaltene molecule that bear a resemblance to the archipelago model is illustrated in figure 9 below. Numerous aromatic rings appear as separate groups that are connected together by several aliphatic chains. However, there is an uncertainty in the model regarding the number of aromatic rings present in the asphaltene molecule. The side chains are thought to have an average length of 5–7 carbons.
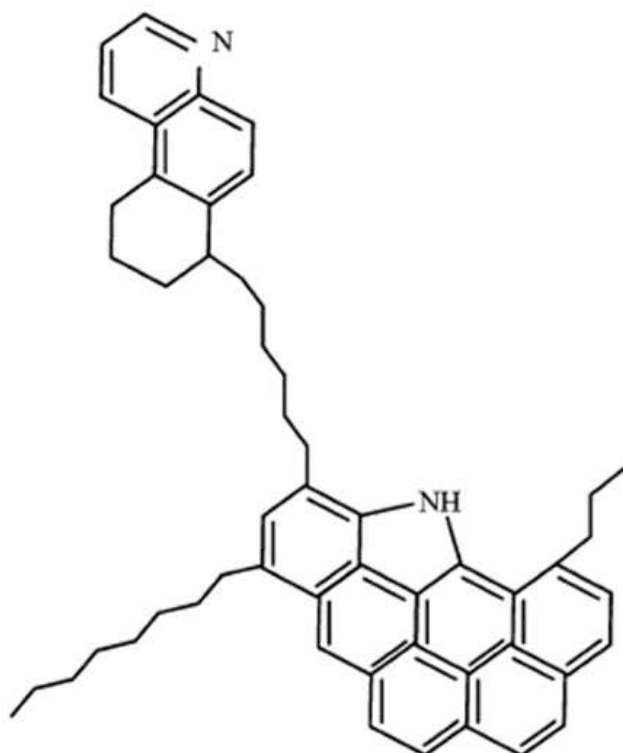
Figure 9 - Archipelago model of asphaltene structure [4]

2.3.2 Continental model

The continental model, also known as the condensed aromatic model, proposes that the structure of an asphaltene molecule is a large group of aromatic rings in the middle of the asphaltene molecule. These rings are linked to several aliphatic branches. This model is usually associated with lower molecular weight asphaltene and is hence referred to as the condensed aromatic model. An illustration of an asphaltene molecule that follows the continental model asphaltene structure is shown in the figure 10 below.
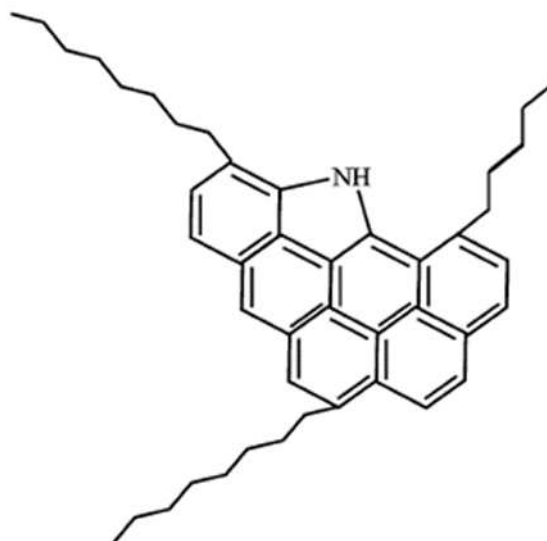
Figure 10 - Continental asphaltene structure [23]

2.3.3 Anionic continental model

The anionic continental model is very similar in structure juxtaposed to that of the continental model. However, unlike the continental model, the anionic continental model has a negatively charged group that is attached to one of the aliphatic chains which is attached to the key structure. Thus, giving the structure of the asphaltene has a negative charge. This negative charge adds to the change in potential of the asphaltene and in turn significantly impacts the stability of the asphaltene stability. This is referred to as the electrokinetic effect.
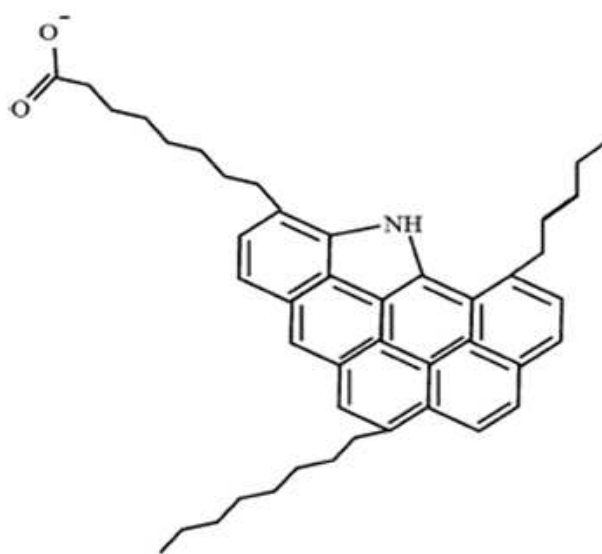
Figure 11. Anionic continental asphaltene structure [23]

17

2.3.4 Yen–Mullins model

Presently, the Yen–Mullins model is the extensively accepted asphaltene model. An illustration of this model is displayed below. This model's description of asphaltene structure is established on size and behaviour as a function of the crude oil in which the asphaltene is contained.

In light oils, with high API gravity, asphaltene molecules are present as small polyaromatic hydrocarbon molecules which have an average diameter of 1.5 nm [11, 27, 39]. In this instance, the concentration of asphaltene is relatively low, and thus, the asphaltene size will not row.

In black oils, with less API gravity relative to light oils, there is an increment in asphaltene concentration, and as a result, the molecules are present in the form of nanoaggregates that have an average diameter of 2 nm. The asphaltene molecules in this case are slightly larger than the asphaltene molecules contained in light oil.

In oils with the lowest API gravity, also known as heavy oils, compared to the aforementioned, the concentration of asphaltene molecules is relatively high and thus leading to the formation of clusters. These clusters formed from the combination if several nanoaggregates and they grow in size and can reach an average diameter of 5 nm.

Generally, the model's description of the presence of asphaltenes shows that, the asphaltene molecule concentration in the oil increases as the oil becomes heavier. Because asphaltenes have a high molecular weight, increment in asphaltene concentration results in decrement in the oil's API. This shows that asphaltene has an overall negative impact on the crude oil. The Yen–Mullins model provides a comprehensive understanding of the size of asphaltene molecules and the probability of its presence in the crude oil.

Figure 12 - Image displaying the different types of asphaltenes present in different types of oils

2.4 Problems associated with asphaltenes

2.4.1 Impact on oil recovery

As previously stated, asphaltenes are solid crude constituents with extremely high molecular weight. However, these molecules are thermodynamically stable and soluble at reservoir conditions. W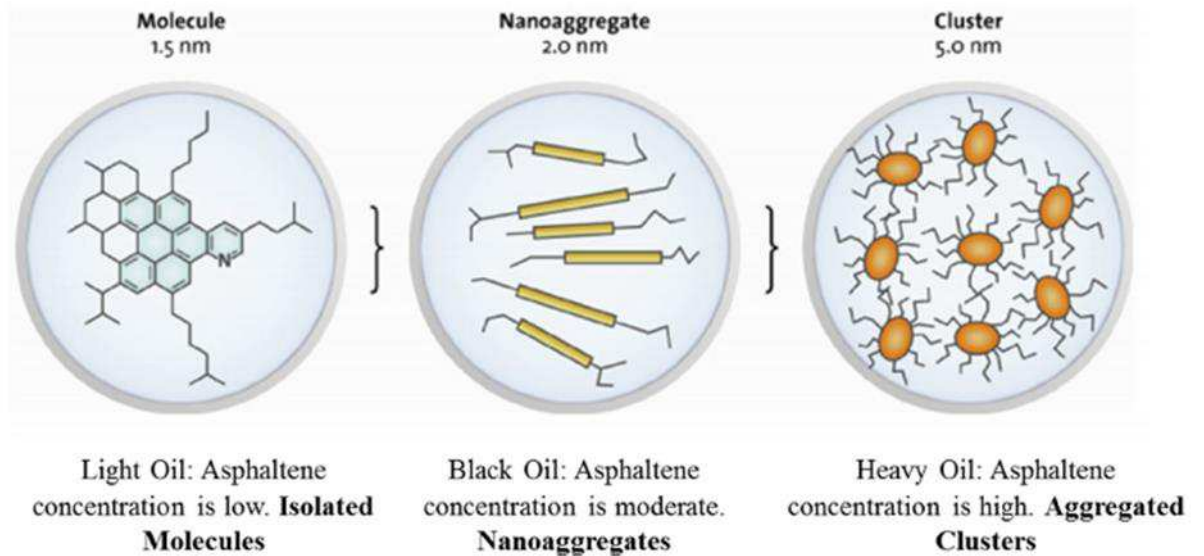hen the reservoir is disturbed, the asphaltene molecules precipitate and combine to form dense asphaltene flocculation. This flocculation, if not noticed early, can deposit themselves into the reservoir pores, wellbores or pipelines resulting in difficulty in the flow. This negatively affects oil recovery.

2.4.2 Asphaltene adsorption and wettability alteration

When there is a great increment in the length of deposition of asphaltene molecules, they begin to adsorb on grain surface of the reservoir, thus engulfing the grains. This then results in the wettability of the oil becoming strongly oil wet which leads to decrements in the relative permeability of the oil and decrease oil recovery.

2.4.3 Alteration of some physical properties of crude oil

The physiochemical properties of crude oils such as the specific gravity (or °API) and viscosity, are influenced predominately by high boiling and heavy weight constituents; considerably the heteroatoms such as sulphur, nitrogen and metals, which are heavily concentrated in asphaltenes. In general, oils with high viscosity and gravity present transportation difficulties. These properties are vital in determining the price of the crude oil. It is thus imperative to characterize the heaviest fractions of crude oils in order to determine their properties and ease of processing. Thus, the need to determine the percent composition of two generally defined classes of compounds, namely resins and asphaltenes.

2.4.4 Coke formation and catalyst deactivation

As already mentioned, asphaltenes are the crude components with the highest molecular weight and as a result, they lead to the formation of coke; a highly carbonaceous product of pyrolysis.

Metals in crude oils are also heavily concentrated in asphaltenes. The problem associated with this is that these metals can contaminate the products as well as depositing themselves on the catalyst thus deactivating the catalyst during catalytic processes. Asphaltenes also can precipitate on surface of processing equipment.

Asphaltene is consequently a solid constituent of crude oil that has an exceptionally high molecular weight [29, 43, 22, 33]. This is chiefly why it is considered to be extremely problematic, because of its ability to form dense flocculation and deposits in reservoir,

wellbores, Storage (sludge and plugging due to further oxidation, among other things) and transportation pipelines. Therefore, it can cause severe operational and production problems.

3.0 Experimental procedure

3.1.0 Sampling

The asphaltene and resin samples that were assessed were isolated from crude oils from two oilfields in the Krasnoyarsk Region. The fields are about 60 km apart. The Oilfields are:
1.   Vankor Oilfield
2.   Quyumba Oilfield
Some properties and group composition of oil from these fields were investigated.

3.1.1 Kinematic viscosity

The determination of the kinematic viscosity was done as per ASTM D445. A clean, calibrated viscometer covering the estimated kinematic viscosity range was selected. The viscometer bath was then adjusted and temperature maintained at 20°C. The Vankor sample was transferred into a capillary tube till the second calibrated test line and inverted. It was then charged into the viscometer using a rubber balloon valve to ensure that moisture does not condense or freeze on the walls of the capillary. The test portion is drowned into the working capillary and timing bulb. By placing rubber stoppers into the tubes to hold the test portion in place and inserting the viscometer into the bath which allows the viscometer to reach bath temperature and remove stoppers. The viscometer holder is connected to the viscometer and then inserted into the transparent bath at 20°C. The charged viscometer was allowed to remain in the bath for 30 minutes. A safe equilibrium time was established by trial because this time will vary for different instruments for different temperature. By adjusting the head level of the test sample to a position in the capillary arm of the instrument 7 mm above the first timing mark, with the samples flowing freely, the flow time was measured in seconds to within 0.1s. The procedure is repeated for a second measurement of flow time. Calculation of the two determination values of kinematic viscosity is done from the measurements of flow time the average of these determined values is used to calculate the kinematic viscosity. Kinematic viscosity at 60°C was also measured and calculated. The procedure was repeated for the Quyumba sample.

3.1.2 Fractional composition

The fractional composition was obtained using GOST standard. A barometer was used to measure the room atmospheric pressure as 740mmHg. 100 mL of the Vankor sample was measured using a measuring cylinder and transferred into a distillation flask. The flask was then placed on the heating mantle in the distillation column and a thermometer attached through the cork of the flask. The heating mantle was turned on and

the initial boiling point was recorded for the sample after which volume of distillates collected at 180 °C, 180-240 °C and 240-360 °C measured. The procedure was repeated for the Quyumba sample.

3.2.0 SARA analysis

Sara analysis was performed according to ASTM D-4124-97. About 15g of sample A was weighed into a flat bottom flask and 300mL of Heptane was added. The mixture was then shaken to obtain a solution using a shaker. The procedure was repeated for sample B and both samples were left to stand overnight for precipitation of asphaltene.
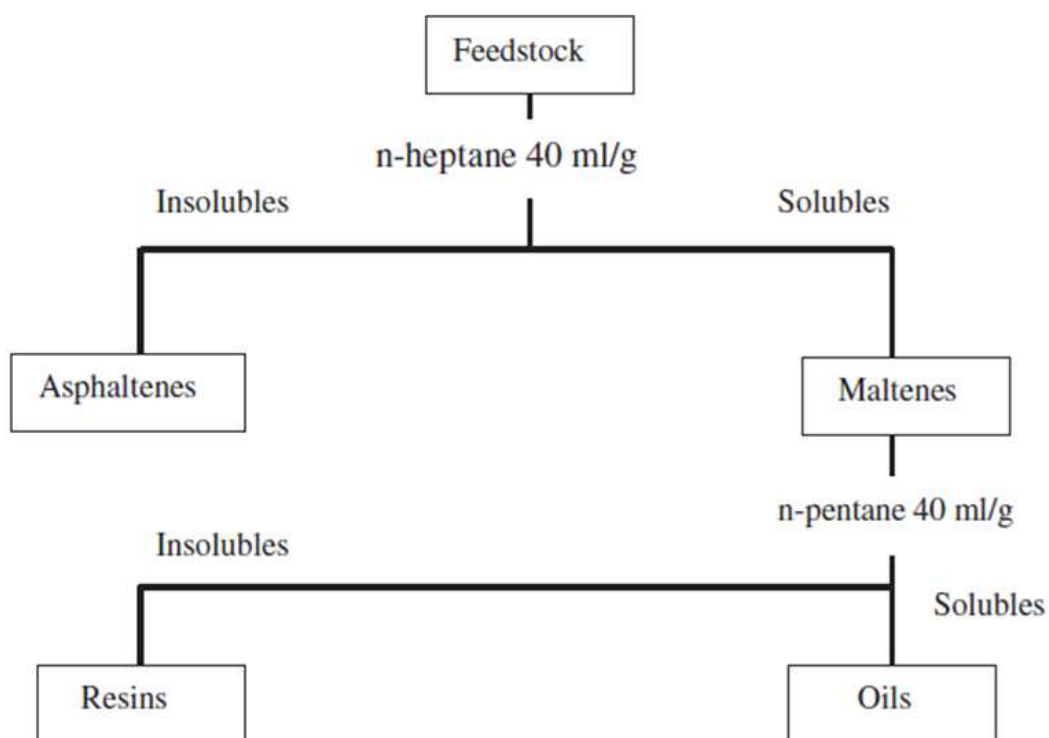
Figure 13 - A flowchart of SARA analysis

A double filter paper was weighed, desiccated and used to separate the precipitated asphaltenes from the maltenes by filtration. The filter paper, holding the asphaltene residue, was then dried for 30 minutes, cooled in the desiccator and weighed. The drying procedure was repeated till a constant weight was obtained and all solvents removed.

The filter paper was then washed using heptane and then the mixture obtained was distilled to obtain the isolated asphaltenes.

After the asphaltenes were isolated, other fractions of crude oil (Saturate, Aromatic and Resin) were separated by column chromatography. A 50mL chromatography column was set up and packed with activated silica gel. About 1g of the maltenes was weighed and 3mL of heptane was added. Small amounts of activated silica gel was then added and

the mixture was dried. The dried silica gel containing the maltenes was then added to the column.

100mL of heptane was used to elute and collect the saturates. 100mL of ethanol was then used to elute and collect aromatics and 100mL of 50 percent volume ethanol and 50 percent volume heptane was used to elute and collect the resins.

Figure 12 - Chromatography column

After the asphaltenes and resins were isolated, they were stored in small plastic containers to prevent absorption of moisture until subsequent analysis were performed by infrared spectroscopy.

3.3.0 Spectroscopic techniques

The infrared and near infrared analysis were performed on the original commercial feedstock samples at 25 °C. A Nicolet 380 FT-IR spectrometer from liquid phase (thin film) was used for the IR analysis. Wavenumbers from 4000 to 400 cm-1 were scanned. The samples were placed in an ATR-cell (Attenuated Total Reflectance) with a potassium

bromide (KBr) crystal. The spectrometer was equipped with a fiber optic sampling probe for transflectance measurements. The wavelength region was set to 1100-2200 nm, and the total number of scans per spectra set to 64. Total path length was 2 mm.
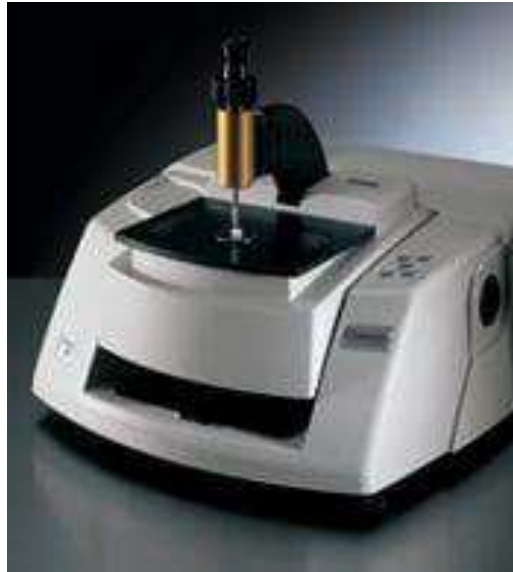
Figure 13 - A Nicolet 380 FT-IR spectrometer

4.0 Results and discussions

4.1.0 Properties of samples

The properties of the samples that were investigated are tabulated in table 2. As can be seen in the table, oil samples from Vankor Field have a higher kinematic viscosity both at 20°C and 60°C than samples from Quyumba Field. This shows that crude oil from Quyumba field flows easily and is less viscous as compared to crude oil from Vankor field. This may be as a result of crude oil from Vankor Field having heavier chemical constituents than Quyumba Field thus increasing its resistance to flow.

The freezing points for both crude oil samples from Vankor and Quyumba Fields were found to be +13°C and -49°C respectively. The inference from this is that hydrocarbon constituent of oil from Vankor field solidify faster than that of Quyumba field as temperatures begin to drop.

The initial boiling point of Vankor crude oil is 73°C while that of Quyumba crude oil is 52°C. This also goes to show that Vankor crude oil is heavier than Quyumba crude oil. It may also be as a result of stronger inter- and intramolecular bonds of constituents of Vankor crude oil. Vankor crude oil has a lower volume percent of gasoline which was recorded as 23.0 vol% compared to the 26.5 vol% of Quyumba Crude oil. Kerosene faction for Vankor crude oil was 39.0 vol% which is 2% more than the 37.0% recorded for Quyumba crude oil and the gas oil faction for both samples were recorded as 35.0 vol% and 36.0 vol% Vankor and Quyumba crudes respectively.

Table 2 - Properties of crude samples analysed

Property	Vankor field	Quyumba field
Kinematic viscosity, mm^2/sec		
at 20 °C at 60 °C	6,14 2,34	5,11 2,13
Freezing point, °C	+13	-49
Fractional composition		
i.b.p. amount of fraction i.b.p.-180 °C, vol% amount of fraction 180-240 °C, vol% amount of fraction 240-360 °C, vol%	73 °C 23,0 39,0 35,0	52 °C 26,5 37,0 36,0

4.1.1 Group composition

The group composition of the samples were also investigated and recorded in table 3. From the table, it can be seen that the percent composition of asphaltenes in Vankor crude oil was found to be 1.4 wt% which is higher than the 1.0 wt% recorded for crude samples from Quyumba. Thus further attesting that Vankor crude oil has higher weight percent of the heavier asphaltene fraction and thus heavier than Quyumba crude oil. It is also noteworthy to mention that Quyumba crude oil has a higher Resin content of 11.8 wt% compared to the 3.5 wt% that was recorded for the Vankor sample. This means that the asphaltenes in Quyumba crudes are well homogenized in the crude oil than in Vankor crude oil and the plausibility of precipitation and deposition should be higher in Vankor crude oil than in Quyumba crude oil under the same conditions. However, Vankor field's crude oil has a higher saturate content of 76.2 wt% than the 67.0 wt% of Quyumba field and the amount of aromatics in recorded was 18.9 wt% and 20.2 wt % for Vankor crude oil and Quyumba crude oil respectively.

Table 3 - Group composition of samples

Content, % wt.	Vankor Field	Quyumba Field
Asphaltenes	1,4	1,0
Resins	3.5	11,8
Saturated (paraffins + naphthens)	76,2	67,0
Aromatic hydrocarbons	18,9	20,2

4.2.0 FTIR spectral analysis of asphaltenes

The FT-IR spectra for asphaltenes of Vankor and Quyumba Oil fields are shown in Figures 14 and 15 respectively and a summary of spectra data are presented in table 4. Detailed FT-IR band assignments for various functional groups have been summarized in appendix A.

For Asphaltene contained in Vankor Crude oil, notable peaks were at 1029,852 cm^{-1} which was assigned to stretching of S=O bond in sulfoxides, 1693,277 cm^{-1} which denoted the stretching of C=O bond in secondary amides and 1604,564 cm^{-1} which was assigned to the stretching of C=C bond in aromatic rings. The adsorption bands at 2750–2950 cm^{-1}, 1440–1450 cm^{-1} and 1375 cm^{-1} can be referred to stretching and deformation

vibrations of saturated C – H bonds and the bands at 3040, 1605, and 700–900 cm⁻¹ correspond to aromatic structures.
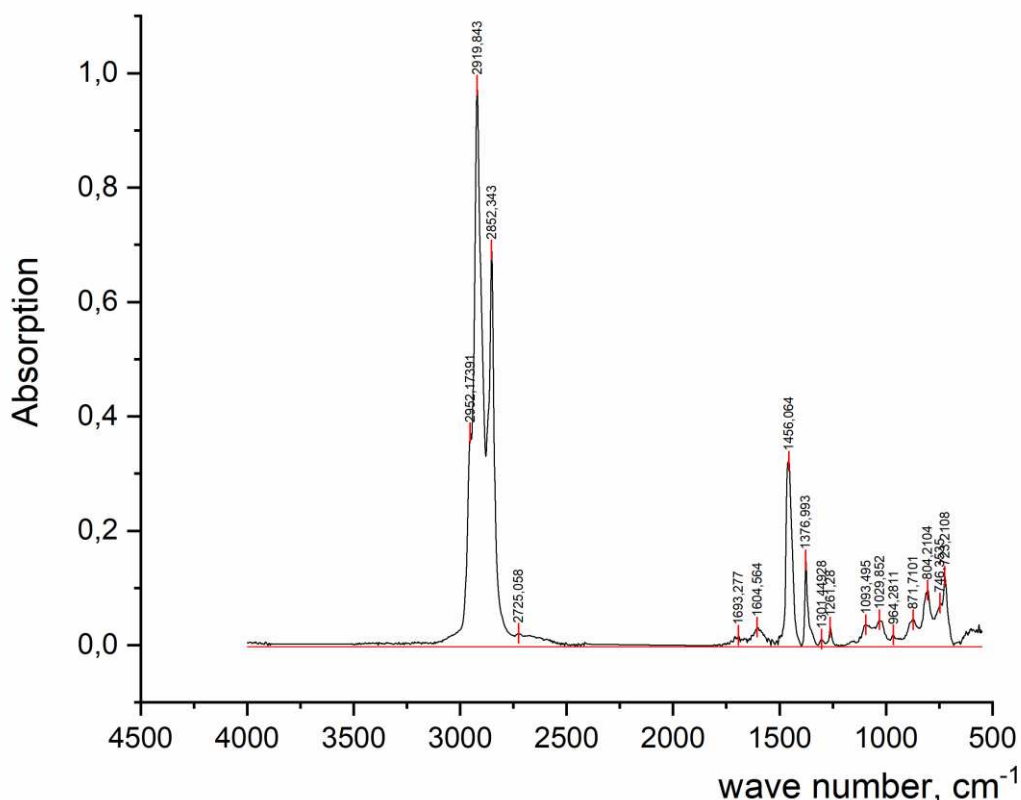
Figure 14 - FT-IR absorption Spectrum for Vankor Asphaltene Sample

Table 4 - Summary of spectral data for asphaltene samples from Vankor Oil Field and Quyumba Field.

Asphaltene Sample	Absorbance										
	742	810	870	1030	1093	1376	1456	1604	2852	2919	2925
Vankor	0.074	0.096	0.044	0.444	0.036	0.149	0.322	0.032	0.691	0.979	0.371
Quyumba	0.065	0.039	0.035		0.007	0.148	0.327	0.024	0.704	0.993	0.373

For asphaltene obtained from crude samples from Quyumba Field, similar peaks were obtained with very few discrepancies. The bands from 900−700 cm⁻¹, which is known as the fingerprint region was similar to the fingerprint region of Vankor asphaltene spectrum. The peaks at 1602,899 cm⁻¹ and 1706,522 cm⁻¹ were also similar to that obtained in the spectrum for the Vankor sample and were assigned to Stretching of C=C bond in aromatic rings and Stretching of C=O bond in secondary amides. However, unlike

27

Vankor, there was no peak at around 1029.852 cm^{-1} to indicate the stretching of S=O bond in sulfoxides.

Another notable difference between both spectra was the absorption intensities of the bands. For instance, for the stretching of C=C bond in aromatic rings band at around 1603 cm^{-1}, the absorption intensity of Vankor field crude oil was 0,03158 while for Quyumba field the absorption was 0,02391. Also, the absorption for the wave number interval of 700 – 900 cm^{-1} for Vankor asphaltene is higher than that of Quyumba asphaltene. This high absorbance is as a result of higher concentration of these bonds.
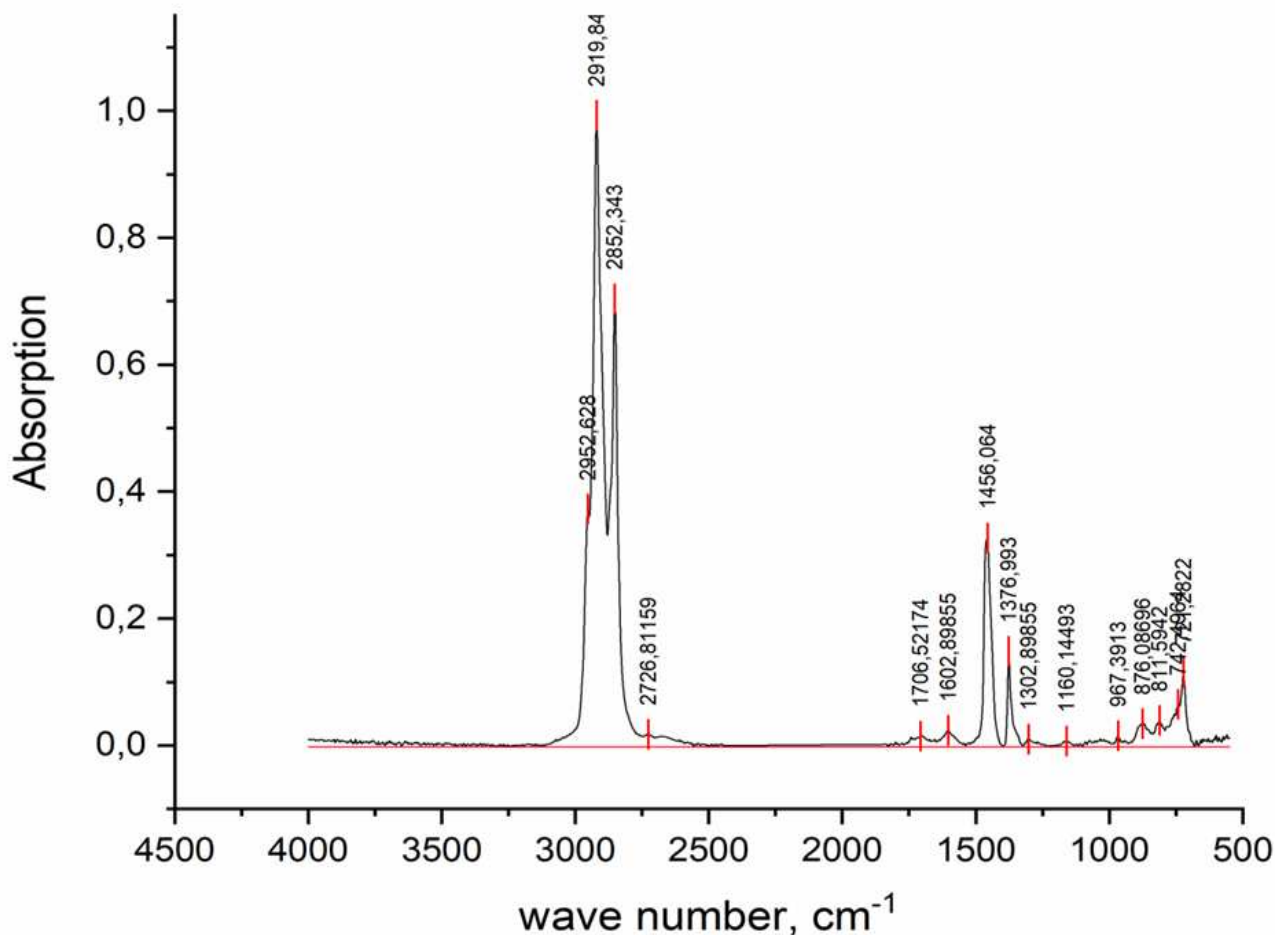
Figure 15 - FT-IR absorption Spectrum for Quyumba asphaltene sample

4.3.1 Deconvolution of Bands in the 3040 – 2720cm^{-1} Region

The FT-IR spectra in the 2720 – 3040 cm^{-1} interval were deconvoluted by Gauss function for a more accurate and precise calculation of the absorption intensity. The results of the deconvolution are presented in figures 16 and 17 while table 5 compares spectra data for both samples. Detailed assignments are presented in Appendix A.

For Vankor crude oil asphaltene, the peak at 2720 cm^{-1} is as a result of the stretching of C–H bonds. There is also a peak at 2850 cm^{-1} and 2890 cm^{-1} which is assigned to

aliphatic symmetrical stretching of C–H bond in CH_3 and asymmetrical stretching of C–H bond in CH_2. The signal at 3040 cm-1 was assigned to aromatic nucleus C−H stretching vibration. Table 6 gives a summary of the wavenumbers, absorbance and assignments.

Model			Gauss			
Equation			y=y0 + (A/(w*sqrt(pi/2)))*exp(-2*((x-xc)/w)^2)			
Plot	Peak1(B)	Peak2(B)	Peak3(B)	Peak4(B)	Peak5(B)	Peak6(B)
y0	-7,05603E-4 ± 0,00483	-7,05603E-4 ± 0,00483	-7,05603E-4 ± 0,00483	-7,05603E-4 ± 0,00483	-7,05603E-4 ± 0,00483	-7,05603E-4 ± 0,00483
xc	2721,01134 ± 23,86537	2850,87887 ± 0,10302	2894,66362 ± 2,05348	2920,11002 ± 0,12772	2956,35567 ± 0,24519	3036,7412 ± 16,83709
w	221,35883 ± 83,32773	16,68626 ± 0,26279	84,2549 ± 2,49262	24,83601 ± 0,30694	17,05857 ± 0,77781	91,61575 ± 43,60406
A	5,16402 ± 3,08137	9,14958 ± 0,19725	41,00026 ± 1,98605	19,29834 ± 0,74593	4,43461 ± 0,40885	1,77802 ± 1,19536
Reduced Chi-Sqr			9,52085E-5			
R-Square (COD)			0,99817			
Adj. R-Square			0,99807			

2720	0,0168
2850	0,4352
2890	0,3884
2920	0,6182
2950	0,2055
3040	0,0168

Figure 16 - Image showing deconvolution of FT-IR absorption Spectrum for the 2720 – 3040 cm-1 interval Vankor Asphaltene Sample

Table 5 - Asphaltene Absorbance and wavenumber for deconvoluted region

Asphaltene Sample	Absorbance					
	2720	2850	2890	2920	2950	3040
Vankor Asphaltene	0.017	0.435	0.388	0.618	0.206	0.017
Quyumba Asphaltene	0.018	0.450	0.393	0.626	0.207	0.014

The deconvolution of the 2720 – 3040 cm^{-1} band for Quyumba field yielded the same results and are detailed in table 7. Again, the difference in the spectra was in the intensities of the peaks. The aliphatic band between 2720 -2950 cm^{-1} for Quyumba asphaltene had higher intensities than that of Vankor asphaltene. However, the aromatic band at 3040 cm^{-1} for Vankor asphaltene has a higher intensity of 0.0168 juxtaposed to the 0.0143 of Quyumba asphaltene. This is as a result of higher aromatic concentration of the Vankor asphaltene whereas Quyumba asphaltene have a higher aliphatic concentration.

Model	Gauss					
Equation	y=y0 + (A/(w*sqrt(pi/2)))*exp(-2*((x-xc)/w)^2)					
Plot	Peak1(B)	Peak2(B)	Peak3(B)	Peak4(B)	Peak5(B)	Peak6(B)
y0	-1,89076E-4 ± 0,00166	-1,89076E-4 ± 0,00166	-1,89076E-4 ± 0,00166	-1,89076E-4 ± 0,00166	-1,89076E-4 ± 0,00166	-1,89076E-4 ± 0,00166
xc	2730,79598 ± 24,25631	2850,71665 ± 0,09562	2895,03948 ± 1,58937	2919,9445 ± 0,11775	2956,22496 ± 0,23447	3035,74541 ± 12,29659
w	191,26071 ± 53,55168	16,58462 ± 0,24463	84,60241 ± 1,86432	24,78309 ± 0,34424	16,98918 ± 0,74091	68,61022 ± 26,25339
A	3,78604 ± 1,32185	9,38359 ± 0,18777	41,62925 ± 1,46421	19,49929 ± 0,61413	4,41575 ± 0,37556	1,06942 ± 0,46047
Reduced Chi-Sqr	8,95686E-5					
R-Square (COD)	0,99823					
Adj. R-Square	0,99814					

2720 0,0182
2850 0,4502
2890 0,3931
2920 0,6263
2950 0,2073
3040 0,0143
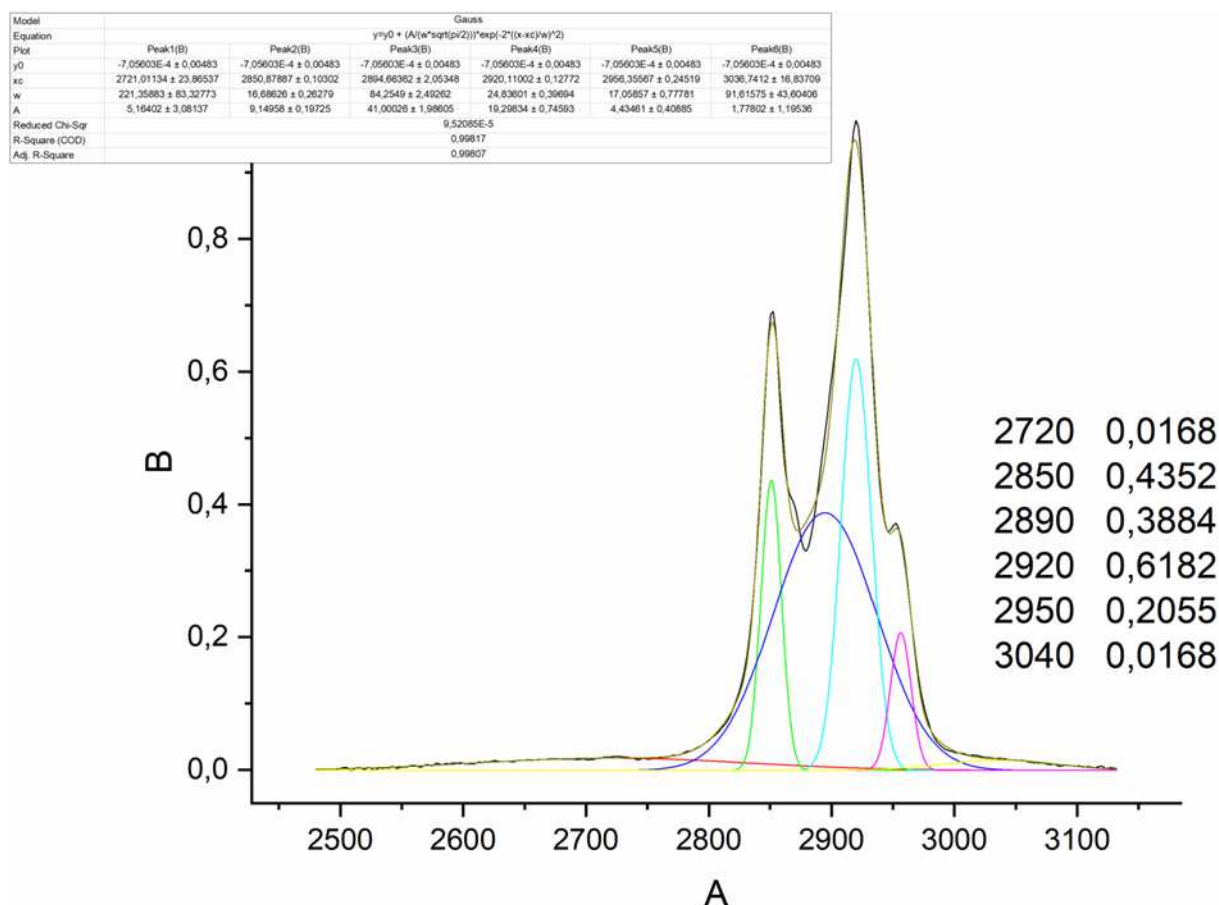
Figure 17 - Image showing deconvolution of FT-IR absorption Spectrum for the 2720 – 3040 cm-1 interval Quyumba Asphaltene Sample.

Some parameters were calculated using the spectral data and are tabulated in table 8 below. The calculations of these parameters are also presented in the appendix B. These parameters that were estimated were used to ascertain differences and similarities between the asphaltene molecules which were investigated.

Table 6 - Parameters evaluated for asphaltene molecular structure of samples from Vankor and Quyumba fields.

Parameter	Sample	
	Vankor	Quyumba
Aromaticity Index by Hydrogen (Har)	0.12	0.10
Aromaticity Index by Carbon	0.65	0.62
Aliphatic Index	0.32	0.31
Long Chain Index	0.26	0.14
Substitution 1 Index	0.21	0.25
Substitution 2 Index	0.37	0.28
Substitution 3 Index	0.46	0.47
Side Alkyl Chain Index	3.28	3.31

From table 8, the calculated value for Aromaticity of the samples by Hydrogen were 0.12 and 0.10 for Vankor and Quyumba samples respectively. This goes to show that the Vankor samples have a higher aromaticity than that of the Quyumba samples. Aromaticity index was estimated again using the intensities of peaks at I_{1607} which corresponds to C=C ring mode stretching peak and I_{1700} represents the intensity of the C=O carbonyl group peak. Again, Vankor had a higher estimation of 0.65 while Quyumba sample was 0.62. The higher aromaticity index indicates that lower carbonyl group that has been substituted at the edges of the molecule. This ratio is also called the maturity index.

The aliphatic index was also estimated as 0.32 and 0.31 for Vankor and Quyumba asphaltene samples respectively. This index is used to determine the presence of aliphatic saturated compounds in the structure of the asphaltene molecule. The difference in the indices was infinitesimal and thus both samples have relatively close aliphatic structures.

The long chain index which is used to determine the carbon number of the aliphatic compounds present in the molecular structure of asphaltene was also estimated. The long chain index for Vankor sample was 0.26 and that for Quyumba field was 0.14. The difference is significant and is indicative of Vankor asphaltene sample's molecular structure has longer chain aliphatic structure juxtaposed to that of Quyumba field.

Substitution 1 Index is an indicator of the benzene structures that share an atom of hydrogen linked to aromatic carbon with other structures. From the estimation, Quyumba samples index of 0.25 suggests that it has more benzene structures sharing an atom of hydrogen linked to aromatic carbon with other structures than the molecular structure of Vankor asphaltene sample which is 0.21.

Substitution 2 Index refers to benzene structures in the molecular structure that share three hydrogen atoms linked to carbon atoms in a benzene ring with other structures. The estimated indices were 0.37 and 0.28 for Vankor and Quyumba samples respectively

and this indicates that the molecular structure of Vankor asphaltene has more of such benzene types.

Substitution 3 Index is an indicator of cata-condensed aromatic structures present in the molecular structure. The estimated values were 0.46 and 0.47 for Vankor and Quyumba samples respectively and the difference here is also minute.

Side Alkyl Chain Index which is also known as ramification degree indicates the side alkyl chains present in the molecular structure. The estimated values were 3.28 and 3.31 for Vankor and Quyumba fields respectively. Thus there is a higher amount of alkyl side chains in the molecular structure of Quyumba field asphaltene compared to that of Vankor field.

4.3.3 FTIR spectra analysis of resins

The FT-IR spectra for resins obtained from Vankor and Quyumba Oil fields are shown in Figures 16 and 17 respectively and detailed FT-IR band assignments for various functional groups have been summarized in Tables 6 and 7.

For resins obtained from Vankor Crude oil, the adsorption bands at $2750-2950 \text{ cm}^{-1}$, $1440-1450 \text{ cm}^{-1}$ and 1376.993 cm^{-1} denote stretching and deformation vibrations of saturated $C-H$ bonds and the bands at 1605, and $700-900 \text{ cm}^{-1}$ correspond to aromatic structures. There was a broad and weak band due to $O-H$ and $N-H$ stretching peaks at $3350,725 \text{ cm}^{-1}$. 1029.71 cm^{-1} which was assigned to stretching of $S=O$ bond in sulfoxides, $1693,478 \text{ cm}^{-1}$ which signifies the stretching of $C=O$ bond in secondary amides and $1605,072 \text{ cm}^{-1}$ which was assigned to the stretching of $C=C$ bond in aromatic rings.
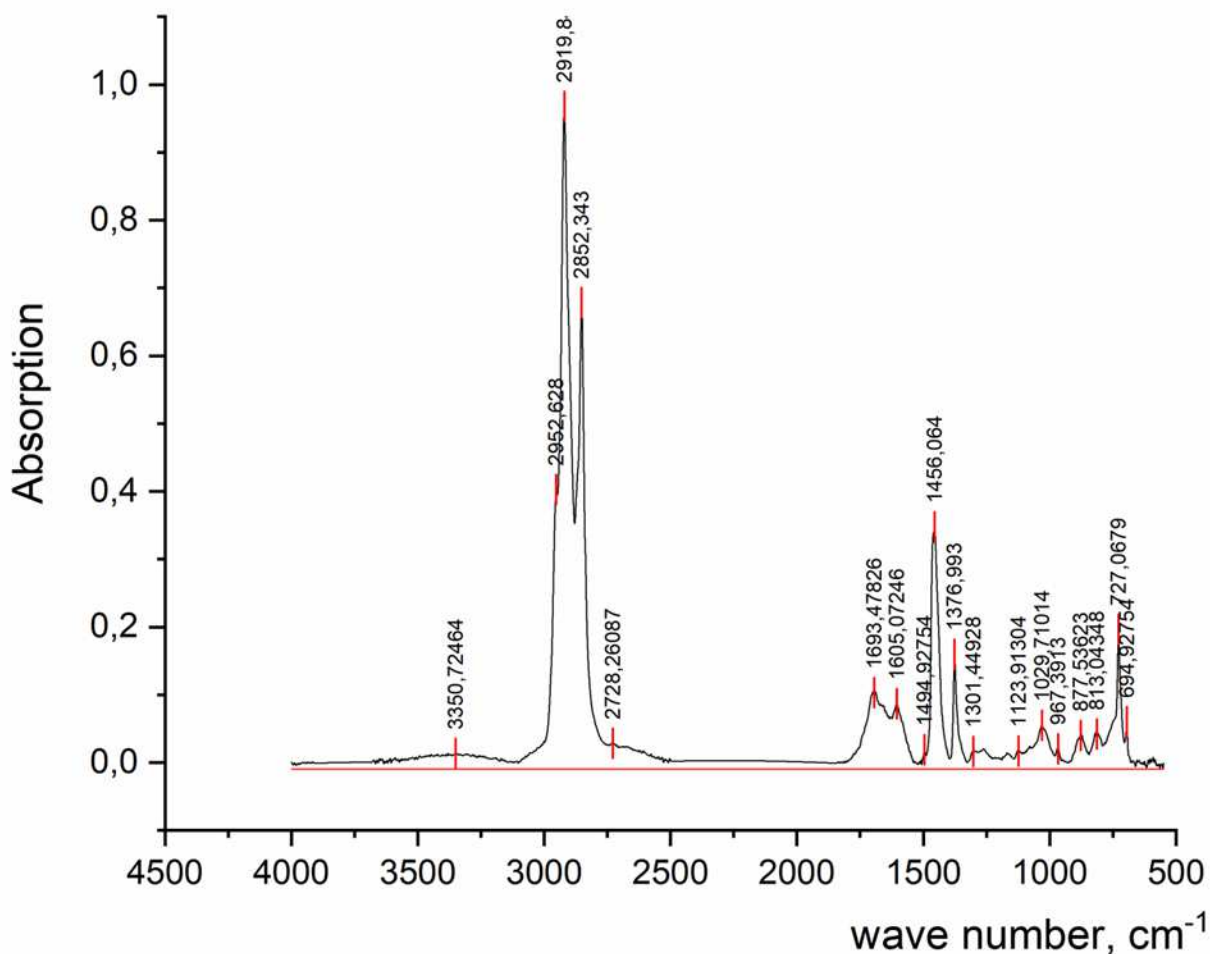
Figure 17 - Image showing FT-IR absorption Spectrum for Vankor Resin Sample.

Table 7 - Summary of spectra data for resin samples from Vankor and Quyumba oil field

Asphaltene Sample	Absorbance										
	742	819	871	1015	1164	1376	1700	2850	2921	2952	3350
Vankor	-	0.042	0.040	0.055	0.017	0.160	0.103	0.679	0.968	0.403	0.014
Quyumba	0.104	0.093	0.046	0.064	0.119	0.177	0.148	0.666	0.975	0.447	0.015

For resins obtained from crude oil samples from Quyumba Field, there was also a broad peak at 3350 cm⁻¹. The peaks at 1598,778cm⁻¹ and 1700,992 cm⁻¹ were also similar to that obtained in the spectrum for the Vankor sample and were assigned to Stretching of C=C bond in aromatic rings and Stretching of C=O bond in secondary amides. There was also a peak at 1015,942 cm-1 to indicate the stretching of S=O bond in sulfoxides.
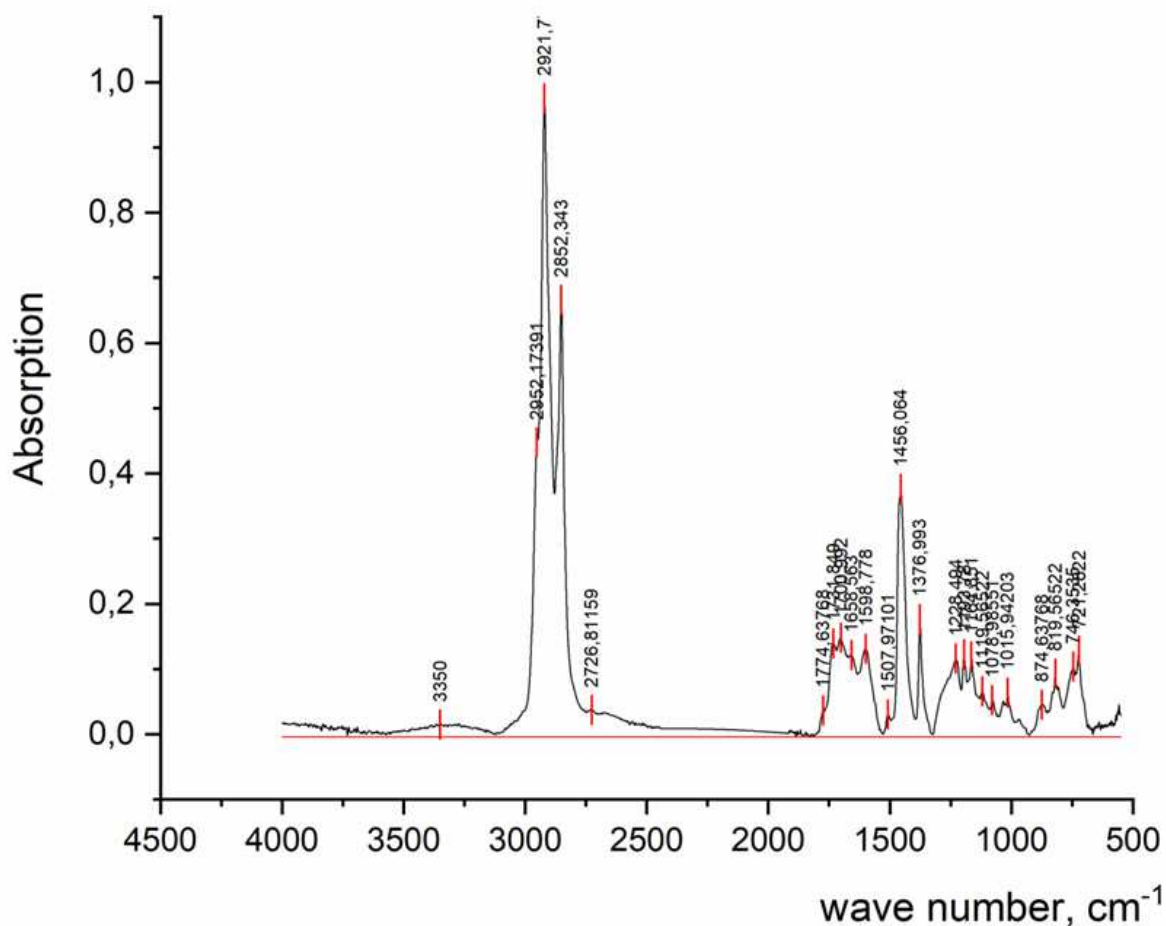
Figure18 - Image showing FT-IR absorption spectrum for Quyumba resin sample.

Some parameters were also calculated using the spectral data and are tabulated in table 8 for the resin samples. The calculations are also presented in the appendix.

Table 8. Parameters evaluated for resin molecular structure of samples from Vankor and Quyumba fields

Parameter	Sample	
	Vankor	Quyumba
Aromaticity Index by Carbon	0.46	0.47
Aliphatic Index	0.29	0.29
Long Chain Index	0.39	0.23
Substitution 1 Index	0.49	0.19
Substitution 2 Index	0.51	0.38
Substitution 3 Index	-	0.43
Side Alkyl Chain Index	2.99	2.18

From table 8, the aromaticity index was estimated as 0.46 and 0.47 for Vankor and Quyumba fields respectively. This shows that the structure of Quyumba resins have more aromaticity than Vankor.

The aliphatic index was also estimated as 0.29 and 0.29 for Vankor and Quyumba resin samples respectively. The difference in the indices was infinitesimal.

The long chain index for Vankor sample was 0.39 and that for Quyumba field was 0.23. The difference is significant and is indicative of the molecular structure of the resin samples from Vankor field having longer chain aliphatic structure compared to that of Quyumba field.

Substitution 1 Index is an indicator of the benzene structures that share an atom of hydrogen linked to aromatic carbon with other structures. From the estimation, Quyumba samples index of 0.25 suggests that it has more benzene structures sharing an atom of hydrogen linked to aromatic carbon with other structures than the molecular structure of Vankor asphaltene sample which is 0.21.

Substitution 2 Index refers to benzene structures in the molecular structure that share three hydrogen atoms linked to carbon atoms in a benzene ring with other structures. The estimated indices were 0.37 and 0.28 for Vankor and Quyumba samples respectively and this indicates that the molecular structure of Vankor asphaltene has more of such benzene types.

Substitution 3 Index is an indicator of cata-condensed aromatic structures present in the molecular structure. The estimated values were 0.46 and 0.47 for Vankor and Quyumba samples respectively and the difference here is also minute.

The estimated side alkyl chain Index were 2.99 and 2.18 for Vankor and Quyumba resin sample respectively. Thus there is a higher amount of alkyl side chains in the molecular structure of Vankor field resin compared to that of Quyumba field.

CONCLUSION

FT-IR spectra was used to elucidate the structures of the asphaltene and resin samples from Vankor and Quyumba oil fields. The aromaticity of Vankor asphaltenes were found to be higher than the aromaticity of Quyumba asphaltenes. However, the reverse was found for the resin molecules where Quyumba resin molecules were estimated to have a higher aromatic. The aliphatic indices suggested that both molecules had only infinitesimal differences in aliphatic structures. The long chain and side alkyl chain indices were higher for both Vankor asphaltene and resin samples and suggests that the molecular structure of those samples have higher alkyl side chains and longer chains than their Quyumba counterparts

REFERENCES

1. Abdel-Raouf M (2012) Factors affecting the stability of crude oil emulsions. In: Crude oil emulsions - composition stability and characterization. Manar El-Sayed Abdel-Raouf, IntechOpen. https://doi.org/10.5772/35018. Available from: https://www.intec hopen.com/books/crude-oil-emulsions-composition-stability-and-characterization/factors-affecting-the-stability-of-crude-oil-emulsions

2. Alshaikh M et al (2018) An innovative dielectric constant measurement method to determine the ideal surfactant candidate to enhance heavy oil recovery. Soc Pet Eng. https://doi.org/10.2118/189752-MS

3. Alshaikh M et al (2019) Anionic surfactant and heavy oil interaction during surfactant-steam process. Soc Pet Eng. https://doi.org/10.2118/195254-MS

4. Alvarez-Ramirez F, Ruiz-Morales Y (2003) Island versus archipelago architecture for asphaltenes: polycyclic aromatic hydrocarbon dimer theoretical studies. Energy Fuels 27(4):1791–1808. https://doi.org/10.1021/ef301522m

5. Bissada KA et al (2016) Group-type characterization of crude oil and bitumen. Part II: efficient separation and quantification of normal-paraffins iso-paraffins and naphthenes (PIN). Fuel 173:217–221

6. Boussingault JB (1837) Mémoire sur la composition des bitumes. Ann Chim Phys 64:141–151

7. Danesh, A., Krinis, D., Henderson, G. D., and Peden, J. M. (1988). Asphaltene deposition in miscible gas flooding of oil reservoirs. Chem. Eng. Res. Des. 66:339

8. Derrick, M.R., Stulik, D., and Landry, J.M., 1999, Infrared Spectroscopy in Conservation Science. The Getty Conservation Institute, Los Angeles, 235 p

9. Fan T et al (2002) Evaluating crude oils by SARA analysis. Presented at the SPE/DOE improved oil recovery symposium, Tulsa, Oklahoma, 13–17 April. SPE-75228-MS

10. Fan H (2003) The effects of reservoir minerals on the composition changes of heavy oil during steam stimulation. J Can Pet Technol 42(3):11–14

11. Forte E, Taylor SE (2014) Thermodynamic modelling of asphaltene precipitation and related phenomena. Adv Coll Interface Sci 217:1–12

12. Garner W, Ham J (1939) The combustion of methane. R Soc A. https://doi.org/10.1098/rspa.1939.0019

13. Goel P et al (2017) Prediction of API values of crude oils by use of saturates/aromatics/resins/asphaltenes analysis: computational-intelligence-based models. Soc Pet Eng J. https://doi.org/10.2118/184391-PA

14. Golkari A, Riazi M (2017) Experimental investigation of miscibility conditions of dead and live asphaltenic crude oil–CO2 systems. J Pet Explor Prod Technol 7:597. https://doi.org/10.1007/s13202-016-0280-4

15. Gregory F. Ulmishek - Petroleum Geology and Resources of the West Siberian Basin, Russia, USGS Bulletin 2201-G, https://pubs.usgs.gov/bul/2201/G/West Siberia structural map

16. Groenzin H, Mullins OC (2000) Molecular size and structure of asphaltenes from various sources. Energy Fuels 14(3):677–684

17. Hirschberg, A., Dejong, L. N. J., Schnipper, B. A., and Meijer, J. G. (1984). Influence of temperature and pressure on asphaltene flocculation. SPE J. 24:283–293

18. https://medlineplus.gov/cholesterol.html (accessed on 6 March 2021)

19. Jha NK et al (2014) Characterization of crude oil of upper Assam field for flow assurance. Presented at the SPE Saudi Arabia Section Annual Technical Symposium and Exhibition, Al-Khobar, Saudi Arabia, 21–24 April. SPE-172226-MS

20. Keshmirizadeh E, Shobeirian S, Memariani M (2013) Determination of saturates, aromatics, resins and asphaltenes (SARA) fractions in Iran crude oil sample with chromatography methods: study of the geochemical parameters. J Appl Chem Res 7(4):15–24

21. Kokal L., Sayegh G (1995) Asphaltenes: The Cholesterol of Petroleum. Paper presented at the Middle East Oil Show, Bahrain, March 1995 https://doi.org/10.2118/29787-MS

22. Kor P et al (2017) Comparison and evaluation of several models in prediction of asphaltene deposition profile along an oil well: a case study. J Pet Explor Prod Technol 7:497. https://doi.org/10.1007/s13202-016-0269-z

23. Kuznicki T et al (2008) Molecular dynamics study of model molecules resembling asphaltene-like structures in aqueous organic solvent systems. Energy Fuels 22(4):2379–2389. https://doi.org/10.1021/ef800057n

24. Lammoglia T, Filho CRdS (2011) Spectroscopic characterization of oils yielded from Brazilian offshore basins: potential applications of remote sensing. Remote Sens Env 115:2525–2535

25. Liao H et al (2019) Effect of crude oil composition on microwave absorption of heavy Oils. Soc Pet Eng. https://doi.org/10.2118/195263-MS

26. Miadonye A, Evans L (2010) The solubility of asphaltenes in different hydrocarbon liquids. Pet Sci Technol J. https://doi.org/10.1080/10916460902936960

27. Mishra VK et al (2012) Downhole fluid analysis and asphaltene nanoscience coupled with VIT for risk reduction in black oil production. Presented at the SPE annual technical conference and exhibition, San Antonio, USA, 8-10

28. Mousavi-Dehghani, S. A., Riazi, M. R., Vafaie Sefti, M., and Mansoori, G. A. (2004). An analysis of methods for determination of onsets of asphaltene phase separations. Journal of Petroleum Science and Engineering 42:145–156.

29. Mozaffari S (2015) Rheology of Bitumen at the onset of asphaltene aggregation and its effects on the stability of water-in-oil emulsion. Master's Thesis, University of Alberta, Canada

30. Mullins OC (2011) The asphaltenes. Ann Rev. Anal Chem 4:393–418

31.   Mullins OC et al (2013) Asphaltene nanoscience and reservoir fluid gradients, tar mat formation, and the oil–water interface. Presented at the SPE annual technical conference and exhibition, Louisiana, USA, 30 Sept 2 Oct

32.   Neumann, H.-J.; Rahimian, I.; Taghizadeh, D. Brenstoff-Chimie 1967, 48, 66.

33.   Nwadinigwe C et al (2015) Studies on precipitation performance of n-heptane and n-pentane/n-heptane on C7 and C5/C7 asphaltenes and maltenes from 350°C atmospheric residuum of three Nigerian light crudes. J Pet Explor Prod Technol 5:403. https://doi.org/10.1007/s13202-014-0150x

34.   Pazuki GR (2007) Application of a new cubic equation of state to computation of phase behavior of fluids and asphaltene precipitation in crude oil. Fluid Phase Equilib 254(1):42–48

35.   Poveda-Jaramillo, J.-C.; Molina-Velasco, D.-R.; Bohorques-Toledo N.-A.; Torres, M.-H.; Ariza-Leon, E. Chemical Characterization of the Asphaltenes from Colombian Colorado Light Crude Oil. Cien. Technol. Fut. 2016, 6, 105-122.

36.   Prakoso AA et al (2017) A mechanistic understanding of asphaltenes precipitation from varying-saturate-concentration perspectives. Soc Pet Eng. https://doi.org/10.2118/177280-PA

37.   Punase A et al (2016) The polarity of crude oil fractions affects the asphaltenes stability. Soc Pet Eng. https://doi.org/10.2118/180423-MS

38.   Rakhmatullin, I.Z.; Efimo, S.V.; Margulis, B.Y.; Klochkov, V.V. Qualitative and Quantitative Analysis of Oil Samples Extracted from some Bashkortostan and Tatarstan Oilfields Based on NMR Spectroscopy Data. J. Petrol. Sci. Eng. 2017, 156, 12-18.

39.   Seifert DJ et al (2012) Black oil, heavy oil, and tar in one oil column understood by simple asphaltene nanoscience. Presented at the Abu Dhabi international petroleum exhibition & conference, UAE, 11–14 November

40.   Seifried C et al (2013) Kinetics of asphaltene aggregation in crude oil studied by confocal laser-scanning microscopy. Energy Fuels 27:1865–1872

41.   Sheu, E. Y., and Storm, D. A. (1995). Colloidal properties of asphaltenes in organic solvents. In Asphaltenes: Fundamentals and applications, Sheu, E. Y. and Mullins, O. (Eds.). New York: Plenum Press, pp. 1–52.

42.   Silva, S.L.; Silva, A.M.S.; Riberio, J.C.; Martins, F.G.; Da Silva, F.A.; Silva, C.M. Chromatographic and Spectroscopic Analysis of Heavy Crude Oil Mixtures with Emphasis in Nuclear Magnetic Resonance Spectroscopy: a Review. Anal. Chim. Acta 2011, 707, 18-37.

43.   Struchkov IA et al (2019) Laboratory investigation of asphaltene induced formation damage. J Pet Explor Prod Technol 9:1443. https://doi.org/10.1007/s13202-018-0539-z

44.   Theyab MA et al (2017) Study of fluid flow assurance in hydrocarbon production—investigation wax mechanisms. PhD Thesis, London South Bank University

45.   Yen, T. F., Erdman, J. G., and Pollack, S. S. (1961). Investigation of the structure of petroleum asphaltenes by X-ray diffraction. Anal. Chem. 33:1587–1593.

Appendix A

Table 9 - Summary of functional group assignment for asphaltene samples from Vankor oil field

Wave Number	Absorption	Assignment
723,2108	0,12073	Out of plane bending of C–H bond in aromatic compounds and bending (rocking type) of C–H in CH_2 (this pick indicate straight chain alkanes with 4 or more carbon atoms)
746,3535	0,07399	Out of plane bending of C–H bond in aromatic compounds
804,2104	0,09617	Out of plane bending of C–H bond in aromatic compounds
871,7101	0,04438	Out of plane bending of C–H bond in aromatic compounds
964,2811	0,01768	
1029,852	0,04442	Stretching of S=O bond in sulfoxides
1093,495	0,03599	In plane bending of C–H bond in aromatic compounds
1261,28	0,03147	
1376,993	0,14933	Symmetrical bending of C–H bond in CH_3
1456,064	0,32171	Aliphatic symmetrical bending of C–H in CH_2, asymmetrical bending of C–H in CH_3 and asymmetrical stretching of C=C bond in aromatic rings
1604,564	0,03158	Stretching of C=C bond in aromatic rings
1693,277	0,01704	Stretching of C=O bond in secondary amides
2725,058	0,02058	Stretching of C–H bond in aldehyde hydrogen
2852,343	0,69108	Symmetrical stretching of C–H bond in CH_3 and asymmetrical stretching of C–H bond in CH_2
2919,843	0,97879	Asymmetrical stretching of C–H bond in CH_2
2952,174	0,37102	Aliphatic CH_3 asymmetric stretching vibration
1301,449	0,01054	Bending of C–H bond in CH3 (wagging and twisting bending) and stretching of C–O bond in carboxylic acid

Table 10 - Summary of functional group assignment for asphaltene samples from Quyumba oil field

Wave Number	Absorption	Assignment
721,2822	0,1152	Out of plane bending of C–H bond in aromatic compounds and bending (rocking type) of C–H in CH_2 (this pick indicate straight chain alkanes with 4 or more carbon atoms)
742,4964	0,0647	Out of plane bending of C–H bond in aromatic compounds
1376,993	0,14816	Symmetrical bending of C–H bond in CH_3
1456,064	0,32709	Symmetrical bending of C–H in $CH2$ ($\delta s\ CH_2$), asymmetrical bending of C–H in $CH3$ ($\delta as\ CH_3$), and asymmetrical stretching of C=C bond in aromatic rings
2852,343	0,70402	Symmetrical stretching of C–H bond in CH_3 and asymmetrical stretching of C–H bond in CH_2
2919,843	0,99278	Asymmetrical stretching of C–H bond in CH_2
2952,628	0,37251	Asymmetrical stretching of C–H bond in CH_3 and stretching of C–H bond in alkanes
811,5942	0,03947	Out of plane bending of C–H bond in aromatic compounds
876,087	0,03454	Out of plane bending of C–H bond in aromatic compounds
967,3913	0,01517	
1302,899	0,00983	Bending of C–H bond in $CH3$ (wagging and twisting bending) and stretching of C–O bond in carboxylic acid
1160,145	0,00678	In plane bending of C–H bond in aromatic compounds
1602,899	0,02391	Stretching of C=C bond in aromatic rings
1706,522	0,01492	Stretching of C=O bond in secondary amides
2726,812	0,01779	Stretching of C–H bond

Table 11. Summary of functional group assignment for deconvolution of 2720 – 3040 cm-1 interval for asphaltene samples from Vankor oil field

Wave Number	Absorption	Assignment
2720	0.0168	Stretching of C–H bond
2850	0.4352	Aliphatic CH_3 symmetric stretching vibration
2890	0.3884	Aliphatic C−H asymmetric stretching vibration
2920	0.6182	Aliphatic CH_2 asymmetric stretching vibration
2950	0.2055	Aliphatic CH_3 asymmetric stretching vibration.
3040	0.0168	Aromatic nucleus C−H stretching vibration

Table 12 - Summary of functional group assignment for deconvolution of 2720 – 3040 cm-1 interval for asphaltene samples from Quyumba oil field

Wave Number	Absorption	Assignment
2720	0.0182	Stretching of C–H bond in aldehyde hydrogen
2850	0.4502	Aliphatic CH_3 symmetric stretching vibration
2890	0.3931	Aliphatic C−H asymmetric stretching vibration
2920	0.6263	Aliphatic CH_2 asymmetric stretching vibration
2950	0.2073	Aliphatic CH_3 asymmetric stretching vibration.
3040	0.0143	Aromatic nucleus C−H stretching vibration

Table 13 - Summary of functional group assignment for resin samples from Vankor oil field.

Wave Number	Absorption	Assignment
727,0679	0,19635	Out of plane bending of C–H bond in aromatic compounds and bending (rocking type) of C–H in CH_2 (this pick indicate straight chain alkanes with 4 or more carbon atoms)
1376,993	0,15971	Symmetrical bending of C–H bond in CH_3
1456,064	0,34745	Symmetrical bending of C–H in CH_2, asymmetrical bending of C–H in CH_3 and asymmetrical stretching of C=C bond in aromatic rings
2852,343	0,67875	Symmetrical stretching of C–H bond in CH_3 and asymmetrical stretching of C–H bond in CH_2
2919,843	0,96789	Asymmetrical stretching of C–H bond in CH_2
2952,628	0,40277	Asymmetrical stretching of C–H bond in CH_3 and stretching of C–H bond in alkanes.
694,9275	0,0602	C-C wagging vibration
813,0435	0,04192	Out of plane bending of C–H bond in aromatic compounds
877,5362	0,03982	Out of plane bending of C–H bond in aromatic compounds
967,3913	0,02063	
1029,71	0,05524	Stretching of S=O bond in sulfoxides
1123,913	0,01704	In plane bending of C–H bond in aromatic compounds
1301,449	0,01649	Bending of C–H bond in CH_3 (wagging and twisting bending) and stretching of C–O bond in carboxylic acid
1494,928	0,01891	Symmetrical bending of C–H in CH_2, asymmetrical bending of C–H in CH_3, and asymmetrical stretching of C=C bond in aromatic rings
1605,072	0,08698	Stretching of C=C bond in aromatic rings

1693,478	0,10305	Stretching of C=O bond in secondary amides
2728,261	0,02862	Stretching of C–H bond
3350,725	0,01352	A broad and weak band due to O–H and N–H stretching

Table 13 - Summary of functional group assignment for resin samples from Vankor oil field.

Wave Number	Absorption	Assignment
721,2822	0,12842	Out of plane bending of C–H bond in aromatic compounds and bending (rocking type) of C–H in CH_2 (this pick indicate straight chain alkanes with 4 or more carbon atoms)
746,3535	0,10361	Out of plane bending of C–H bond in aromatic compounds
1164,851	0,11933	In plane bending of C–H bond in aromatic compounds
1193,78	0,12309	
1228,494	0,11585	
1376,993	0,17658	Symmetrical bending of C–H bond in CH_3
1456,064	0,37602	
1598,778	0,13083	Stretching of C=C bond in aromatic rings
1658,563	0,12142	
1700,992	0,148	Stretching of C=O bond in secondary amides
1731,849	0,13954	
2852,343	0,66637	Symmetrical stretching of C–H bond in CH_3 and asymmetrical stretching of C–H bond in CH_2
2921,771	0,97549	Asymmetrical stretching of C–H bond in CH_2
819,5652	0,09288	Out of plane bending of C–H bond in aromatic compounds
874,6377	0,04553	Aromatic nucleus (CH), one adjacent H deformation
1015,942	0,06382	Stretching of S=O bond in sulfoxides
1078,986	0,05209	Phenolic deformation (C−O−C) (stretching)
1119,565	0,06563	
1507,971	0,03062	Symmetrical bending of C–H in CH_2, asymmetrical bending of C–H in CH_3, and asymmetrical stretching of C=C bond in aromatic rings
1774,638	0,03698	
2726,812	0,03736	Stretching of C–H bond
2952,174	0,44737	Aliphatic CH_3 asymmetric stretching vibration
3350	0,01515	A broad and weak band due to O–H and N–H stretching

Appendix B

1. Calculation for Aromaticity Index by Hydrogen

$$H_{ar} = \frac{A^{3050}/0.2 \times A^{2920}}{1 + (A^{3050}/0.2 \times A^{2920})}$$

(a) For Vankor Asphaltene sample:

$$H_{ar} = \frac{0.0618/0.2 \times 0.6182}{1 + (0.0618/0.2 \times 0.6182)} = 0.1196$$

44

(b) For Quyumba Asphaltene sample:

$$H_{ar} = \frac{0.0143/0.2 \times 0.6182}{1 + (0.0143/0.2 \times 0.6182)} = 0.1025$$

2.   **Calculation of Aromaticity Index (AI)**

$$AI = \frac{I_{1607}}{I_{1607} + I_{1700}}$$

(a) For Vankor Asphaltene sample:

$$AI = \frac{0.0316}{0.0316 + 0.0174} = 0.650$$

(b) For Quyumba Asphaltene sample:

$$AI = \frac{0.0239}{0.0239 + 0.0149} = 0.616$$

(c) For Vankor Resin sample:

$$AI = \frac{0.087}{0.087 + 0.1031} = 0.4577$$

(d) For Quyumba Resin sample:

$$AI = \frac{0.1308}{0.1308 + 0.148} = 0.4692$$

3.   **Calculation for Aliphatic Index (ALI)**

$$ALI = \frac{A_{1460} + A_{1376}}{A_{1700} + A_{1600} + A_{1376} + A_{1030} + A_{864} + A_{814} + A_{743} + A_{724} + A_{2953} + A_{2862}}$$

(a) For Vankor Asphaltene sample:

$$ALI = \frac{0.3217 + 0.1493}{0.017 + 0.0316 + 0.1493 + 0.0444 + 0.0444 + 0.0962 + 0.074 + 0.1207 + 0.3710 + 0.6911} = 0.316$$

(b) For Quyumba Asphaltene sample:

$$ALI = \frac{0.3271 + 0.1482}{0.0149 + 0.0239 + 0.1482 + 0 + 0.0345 + 0.0395 + 0.0647 + 0.1152 + 0.3725 + 0.7040} = 0.313$$

(c) For Vankor Resin sample:

$$ALI = \frac{0.3475 + 0.1597}{0.1031 + 0.087 + 0.1597 + 0.0553 + 0.0398 + 0.0419 + 0 + 0.1964 + 0.4028 + 0.6788} = 0.2874$$

(d) For Quyumba Resin sample:

$$ALI = \frac{0.3760 + 0.1766}{0.01214 + 0.1308 + 0.1766 + 0 + 0.0455 + 0.0929 + 0.1036 + 0.1284 + 0.4474 + 0.664} = 0.2889$$

4. Calculation for Long Chain Index (LCI)

$$LCI = \frac{A_{724}}{A_{1460} + A_{1376}}$$

(a) For Vankor Asphaltene sample:

$$LCI = \frac{0.1207}{0.3217 + 0.1493} = 0.2563$$

(b) For Quyumba Asphaltene sample:

$$LCI = \frac{0.0647}{0.3271 + 0.1482} = 0.1361$$

(c) For Vankor Resin sample:

$$LCI = \frac{0.1964}{0.3475 + 0.1597} = 0.3872$$

(d) For Quyumba Resin sample:

$$LCI = \frac{0.1284}{0.3760 + 01766} = 0.2323$$

5. Substitution 1 Index (Subs1)

$$Subs1 = \frac{A_{864}}{A_{814} + A_{864} + A_{743}}$$

(a) For Vankor Asphaltene sample:

$$Subs1 = \frac{0.444}{0.0962 + 0.0444 + 0.074} = 0.2069$$

(b) For Quyumba Asphaltene sample:
$$Subs1 = \frac{0.0345}{0.0395 + 0.0345 + 0.0647} = 0.2487$$

(c) For Vankor Resin sample:
$$Subs1 = \frac{0.0398}{0.0419 + 0.0398 + 0} = 0.487$$

(d) For Quyumba Resin sample:
$$Subs1 = \frac{0.0455}{0.0929 + 0.0455 + 0.1036} = 0.188$$

6. Substitution 2 Index (Subs 2)
$$Subs2 = \frac{A_{814}}{A_{814} + A_{864} + A_{743}}$$

(a) For Vankor Asphaltene sample:
$$Subs2 = \frac{0.0962}{0.0962 + 0.0444 + 0.1207} = 0.3682$$

(b) For Quyumba Asphaltene sample:
$$Subs2 = \frac{0.0395}{0.0395 + 0.0345 + 0.0647} = 0.2848$$

(c) For Vankor Resin sample:
$$Subs2 = \frac{0.0419}{0.0419 + 0.0398 + 0} = 0.487$$

(d) For Quyumba Resin sample:
$$Subs2 = \frac{0.0929}{0.0929 + 0.0455 + 0.1036} = 0.384$$

7. Calculation for Substitution 3 (Subs 3)
$$Subs3 = \frac{A_{743}}{A_{814} + A_{864} + A_{743}}$$

(a) For Vankor Asphaltene sample:
$$Subs3 = \frac{0.1207}{0.0962 + 0.0444 + 0.1207} = 0.4619$$

(b) For Quyumba Asphaltene sample:
$$Subs3 = \frac{0.0647}{0.0395 + 0.0345 + 0.0647} = 0.4665$$
(c) For Vankor Resin sample:
$$Subs3 = \frac{0}{0.0419 + 0.0398 + 0} = -$$
(d) For Quyumba Resin sample:

$$Subs3 = \frac{0.1036}{0.0929 + 0.0455 + 0.1036} = 0.4281$$

8.   Calculation for Side Alkyl Chain (SAC) using constant K = 1.243
$$SAC = K \times \frac{I_{2927}}{I_{2957}}$$
(a) For Vankor Asphaltene sample:
$$SAC = 1.243 \times \frac{0.9788}{0.3710} = 3.2794$$
(b) For Quyumba Asphaltene sample:
$$SAC = 1.243 \times \frac{0.9928}{0.3725} = 3.3129$$
(c) For Vankor Resin sample:
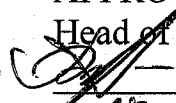$$SAC = 1.243 \times \frac{0.9679}{0.4028} = 2.9868$$
(d) For Quyumba Resin sample:
$$SAC = 1.243 \times \frac{0.9755}{0.4744} = 2.710$$

Federal State Autonomous Educational Institution of
Higher Education
"SIBERIAN FEDERAL UNIVERSITY"
School of Petroleum and Natural Gas Engineering
Department of Chemistry and Technology of
Natural Energy Carriers and Carbon Materials

APPROVED
Head of the Department
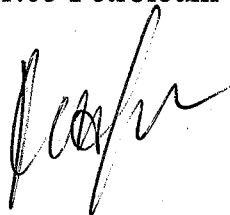Fedor.A. Buryukin
« 25 » 06 2020 г.

MASTER'S THESIS

Investigations of Asphaltenes' Structure and Properties of West Siberian Crude Oils

04.04.01 Chemistry
04.04.01.05 Petroleum Chemistry and Refining

Research supervisor   Candidate of   Vladimir Safin
Chemical Sciences,
Associate Professor

Graduate   Asamoah A.Abraham

Krasnoyarsk 2021